OPTIMIZATION OF CARBON NANOTUBE SUPERCAPACITOR ELECTRODE

By

Serkan Akbulut

Thesis

Submitted to the Faculty of the

Graduate School of Vanderbilt University

in partial fulfillment of the requirements

for the degree of

MASTER OF SCIENCE

in

Electrical Engineering

August, 2011

Nashville, Tennessee

Approved:

Professor W. P. Kang

Professor Jimmy L. Davidson

To my family

ACKNOWLEDGEMENTS

First of all, I would like to thank my academic and research advisor, Prof. W.P. Kang for his assistance, guidance and encouragement throughout my study at Vanderbilt University. I would like to thank Mr. Supil Raina, S. Wei and Nikkon Ghosh for their diverse discussions and assistance in my work. I am also thankful to my colleagues to keep the work going.

Finally I would like to express my sincere appreciation for my parents, my sister, and my uncle-aunty, whose constant support made me persistently strong during difficult moments.

TABLE OF CONTENTS

Page

ABSTRACT

Carbon nanotubes (CNTs) have many potential applications due to their electrical conductivity, excellent chemical properties, mechanical strength, and high surface area. Because of their unique material properties, CNTs are promising for next generation supercapacitor applications. CNTs based electrode offers exceptional energy and power performance due to the high surface area and the ability to functionalize the CNTs to optimize electrochemical supercapacitor properties.

This research is focused on the synthesis of CNTs and electrochemical characterization of CNTs based electrode to improve the performance of ultracapacitors. In brief, the $H_2/NH_3/CH_4$ (75:75:25 sccm) and $H_2/NH_3/CH_4$ gas mixture (75:100:25 sccm) for different growth time (2, 4, 6, 8, and 10 min) were applied to CNT synthesis using HFCVD. Growth characteristics of carbon nanotubes changed from spaghetti-like to vertical aligned when the growth condition was switched from low to high ammonia ratio. The length of carbon nanotubes changed from ~2 μm to ~50 μm when the growth time lengthened.

Post synthesis treatment of CNTs including polyvinyl alcohol (PVA) treatment, H_2O_2 (hydrogen peroxide) treatment, H_2 (hydrogen) plasma treatment, were performed and used to improve the CNTs electrodes capacitance. The encouraging results demonstrated that polyvinyl alcohol (PVA) could be used to functionalize carbon nanotubes and transform the as grown hydrophobic nanotube surfaces into desirable hydrophilic surface to enhance the capacitive performance. On the other hand, both hydrogen peroxide treatment and hydrogen plasma treatment were found not to be useful for modifying the carbon nanotubes for ultracapacitor application.

LIST OF TABLES

LIST OF FIGURES

CHAPTER I

INTRODUCTION

Carbon Nanotubes

Carbon nanotubes (CNTs) are new form of carbon allotropes with cylindrical hollow nanostructures and high length-to-diameter aspect ratio [1]. Since the discovered of carbon nanotubes (CNTs) by Iijima in 1991 [2], research progress has been made toward many applications such as energy storage devices, fuel cells, lithium ion batteries, transistors, sensors, and field emission devices [2].

The structure of nanotubes is visualized in terms of chirality, which is formed by rolling over a graphene sheet described by a vector $\boldsymbol{C}_h$ in terms of two integers (n,m) related to graphite lattice vectors $\mathbf{a_1}$ and $\mathbf{a_2}$ (Figure 1.1) [3]. The chiral vector can be described by the following equation:

$$\boldsymbol{C}_h = n\mathbf{a_1} + m\mathbf{a_2} \quad \text{.....1.1}$$

Three different types of nanotube structures can be created by rolling up the graphene sheet into a cylinder as shown in Figure 1.1 [2]. The armchair and zigzag nanotubes, respectively, with chiral angles of $\Theta = 0$ and 30°, and the chiral nanotubes with $0 < \Theta < 30°$ [4], for zigzag (m = 0) and armchair (m = n). Note that $n \geq m$ is used for convention [5].

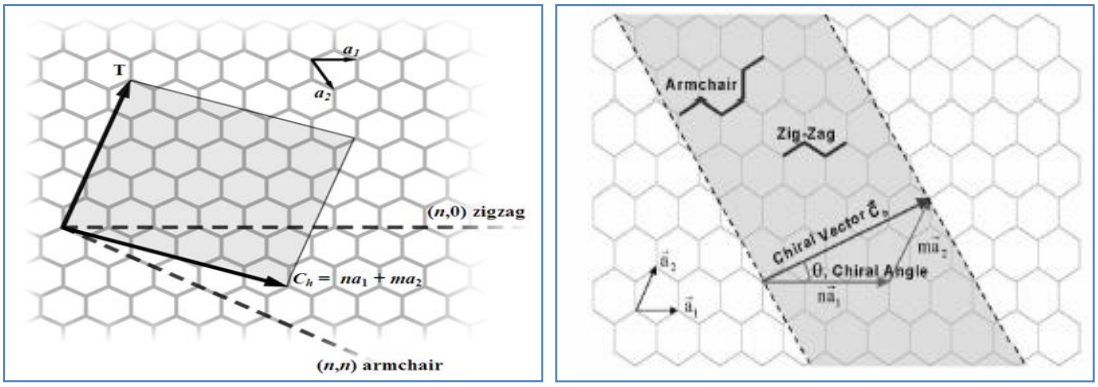

Figure 1.1: (a) A nanotube (n,m) is created by rolling a graphite sheet along the chiral vector $\boldsymbol{C_h}$ = n$\mathbf{a_1}$ + m$\mathbf{a_2}$ on the graphite where $\mathbf{a_1}$ and $\mathbf{a_2}$ are graphite lattice vector, (b) Showing hexagonal sheet of graphite is rolled to form a carbon nanotube.

Carbon, which has a low atomic number, is the sixth element in the periodic table [6]. Each carbon atom has six electrons occupying 1s2, 2s2 and 2p2 atomic orbitals. The 1s2 orbital includes two bound core electrons. Shifting the occupation of the 2s and three 2p atomic orbitals can enhance the binding energy of the C atom with its dwelling atoms. The combining of 2s and 2p atomic orbitals is called hybridization. There are three hybridizations in carbon such as sp, sp2 and sp3. [6]

Carbon nanotubes are generally observed in one of the two forms [80], multiwalled or single-walled [7], which were found in 1991 and 1993, respectively. Single-walled carbon nanotubes (SWNTs) have cylindrical walls with diameters ranging between 1 and 3 nm [6]. The tube can be envisioned as a hollow cylinder, formed by rolling over graphene sheet, as shown in Figure 1.2 [5]. Multiwalled carbon nanotubes (MWNTs) have thicker and nested coaxial walls, consisting of several coaxial graphene cylinders separated by spacing (0.34 nm) that is close to the interlayer distance in graphene [6].

Carbon nanotubes were discovered in the early 2000s [8]. Carbon nanotubes are becoming very popular due to their electrical conductivity, excellent chemical properties, and mechanical strength. Potential applications of CNTs include batteries for cell phones and cars [9], chemical sensors for security systems [10], hydrogen storage for electrochemical devices [11], electron field emitter for flat panel displays [12] and vacuum field emission displays [13], electron source for vacuum electronics [14], microwave power amplifier for space electronics [15], gas sensors for chemical sensing [15], scanning probe for atomic force microscope (AFM) [16], wires for quantum electronics [17], hydrogen storage for fuel cells [18], electrodes for discharge tubes [19], electrochemical capacitor for energy storage [20], nonvolatile random access memory for molecular computing [21], nanotweezers for microelectromechanical systems (MEMS) [22], and semiconductor for solid state nanoelectronics [23].

The next decade will be the era of nanotechnology thus requiring research in nanotubes. Carbon nanotubes and their products will play an important role in the advance of nanotechnology. Large amounts of resources have been invested for understanding and developing the carbon nanotube material. Overall, the volume of nanotube research is growing, and commercial applications will not be far behind [24].

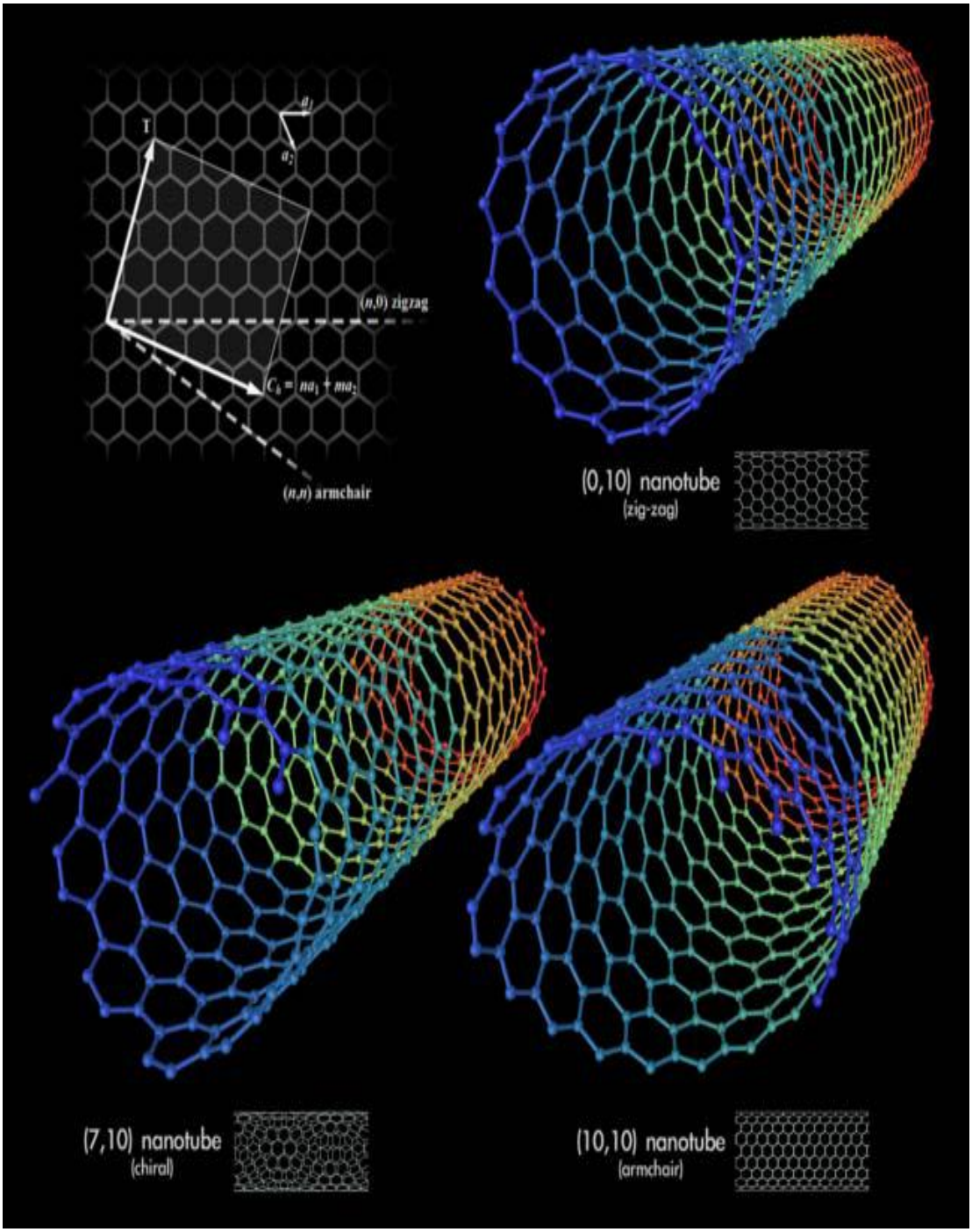

Figure 1.2: 3D model of three types of single-walled carbon nanotubes. By rolling a graphite sheet in different directions, these typical configurations can be obtained: zigzag (n, 0), armchair (n, n) and chiral (n, m) where n>m>0 by definition. In this specific example, they are (10, 0), (10, 10) and (7, 10) respectively.

Carbon Nanotube Based Electrochemical Supercapacitors

Supercapacitors, also known as electrochemical double layer capacitors, or ultracapacitors, have tremendous potential as high energy and high power storage devices. The first approach for supercapacitors was based on porous carbon material with high surface area. The first patent on supercapacitors was awarded in 1957 [25].

In 1969, SOHIO marketed such an energy storage device using high surface area carbon materials as the electrode with tetraalkylammonium salt as the electrolyte [25]. SOHIO went on to patent a disc-shaped capacitor in 1970 utilizing a carbon paste soaked in an electrolyte [25]. In 1971, NEC (Nippon Electric Company) produced the first commercially successful double-layer capacitors under the name "supercapacitor." These low voltage devices had a high internal resistance and were thus primarily designed for memory backup applications, finding their way into various consumer appliances. Matsushita Electric Industrial (Panasonic, Japan) developed Gold capacitors in 1978. These devices were also intended for use in memory backup applications. In 1982, the first high-power double-layer capacitors were developed by PRI (Pinnacle Research). These devices were designed for military applications such as laser weaponry and missile guidance systems. Large numbers of supercapacitor patents have been granted as cited by Sarangapani in 1996 [25]. Supercapacitors have recently been considered as energy storage devices for hybrid electric vehicles and renewable energy sources [25].

In parallel plate capacitor, the capacitance varies inversely on the inter electrode separation [26]. In supercapacitor, capacitance depends on the separation between the charge on the electrode and the countercharge in the electrolyte [26], which is much smaller than plate separation of the dielectric capacitor.

Typically, the capacitance of a supercapacitor is ~1000 times higher than the regular dielectric capacitor, and its power density is ~100 times higher than batteries. A comparison of the properties, performance and efficiency between supercapacitor, dielectric capacitor and battery is given in Table 1.1 [27].

Table 1: Comparison of Capacitor, Supercapacitor and Battery

Parameters	**Dielectric Capacitor**	**Supercapacitor**	**Battery**
Charge Time	10^{-6}~10^{-3} sec	1-30 sec	3~4 hrs
Discharge Time	10^{-6}~10^{-3} sec	1-30 sec	1 ~ 5 hrs
Energy Density (Wh/kg)	< 0.1	1 ~ 10	20 ~ 100
Power Density (W/kg)	> 10,000	1,000 ~ 2,000	50 ~ 200
Cycle life	> 500,000	> 100,000	500~2000
Charge/Discharge Efficiency	~ 1.0	0.90 ~ 0.95	0.7~ 0.85

Having high energy and high discharge time make supercapacitors superior to dielectric capacitors. Due to absence of chemical reactions, supercapacitors have longer cycle life compared to batteries. Even though batteries have the highest energy density compared to dielectric capacitors and supercapacitors, they have the lowest power density and cycle life [28].

Recent studies have shown that the advantages of supercapacitors are more than their disadvantages. Some of the advantages and disadvantages [28] of supercapacitors are:

Advantages

- Provides backup power
- Fast charging.
- Unlimited cycle life, over > 100,000.
- Quick mode of operation.
- Very low impedance.
- Excellent reversibility.
- Simple charge methods.
- Reduces battery size
- Minimizes space requirements
- Allows low/high temperature operation

Disadvantages

- Low energy density.
- Linear discharge voltage prevents use of the full energy spectrum

- Required high self-discharge.
- Needed serial connection to obtaining high voltages
- Voltage balancing is required if more than three capacitors are connected in series
- Required sophisticated electronic control and switching equipment

In recent years, many new supercapacitor electrode materials have been investigated, including conductive polymers (polythiophene [29], polypyrrole [30], polyaniline [31]), metal oxides (RuO_2, IRO_2, MnO_2 [25]), and different types of carbon materials (carbon aerogel, activated carbon, carbon nanotubes [25]).

Due to high surface area ~ 1000 to 2000 m^2/g, carbon materials are the preferred material for supercapacitor electrodes. Carbon materials studied in recent years for this application include carbon black, carbon cloth, carbon aerogels, and CNTs [25].

The specific capacitance of the carbon nanotubes can be varied from 20 F/g to 300 F/g, depending on method of fabrications and electrode configurations. The first reported MWNT supercapacitor electrodes prepared by Niu et al has specific capacitance, energy density and power density of 113 F/g, 0.56 Wh/kg and 8 kW/kg, respectively [25]. CNT-based supercapacitors have higher energy density and higher power density compared to traditional electrochemical capacitors, as shown Figure 1.3 [32].

Carbon nanotubes are very attractive both for industrial and academic research due to their unique properties. The electronic conductivity, mechanical

properties, optical properties, and thermal conductivity of carbon nanotubes are very impressive.

Based on these properties, many applications or potential applications have been reported for carbon nanotubes [25], such as high-strength composites, hydrogen storage media, energy storage and energy conversion devices, field emission displays, radiation sources, nano-sized semiconductor devices, and sensor probes [25].

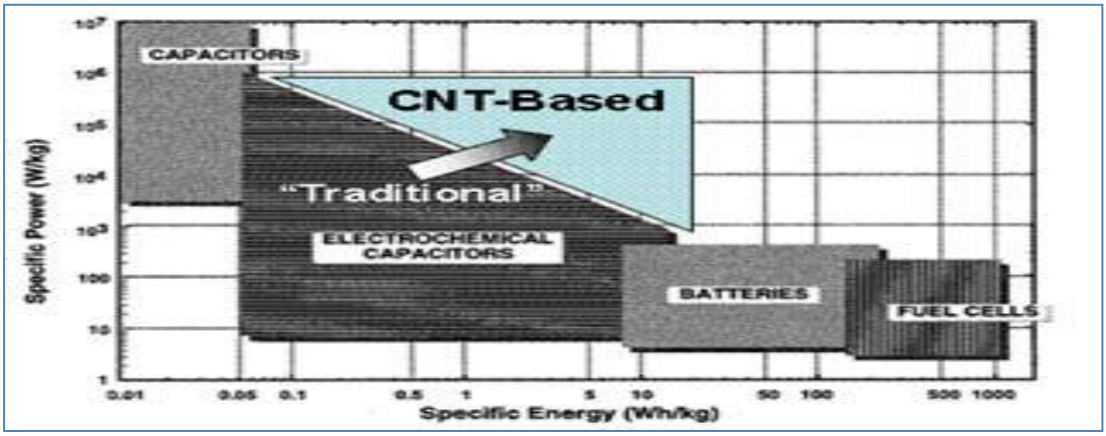

Figure 1.3: Plot of specific power versus specific energy for various power/energy sources.

Chemical activation and physical treatment can be used to improve the specific surface area of CNTs-based electrodes by introducing micropores to enhance the capacitance performance. Chemically and physically activated [25] carbon nanotubes electrodes were found to have higher specific area and specific capacitance over non-activated electrodes [25].

The wetting capability of CNT electrode affects the capacitance behavior. For this reason, the hydrophilic or hydrophobic property of carbon nanotubes is getting attention in CNT-based electrochemical supercapacitors.

Various activation and treatment processes such as nitric acid treatment (HNO_3) [33], fluorine [34] gas activation, ammonia plasma treatment (NH_3) [35], hydrogen plasma treatment [36], hydrogen peroxide treatment (H_2O_2) [37], photo oxidation treatment [38], and sulfuric acid treatment (H_2SO_4) [39] have been studied for enhancing the capacitance performance of carbon nanotubes. However, some of the treatment methods such as sulfuric acid and hydrogen plasma treatments [39] have led to unstable capacitance and current leakage.

Conducting polymers, such as polyvinyl alcohol, polypyrrole, polyacetylene, polyaniline, polythiophene, and their derivatives are also common electrode materials that scientist used in recent years for supercapacitor applications [25]. The incorporation of CNTs with conducting polymers increases the capacitance of the composite due to redox reactions contributed by the conducting polymers [25]. CNTs are electron acceptors, when the conducting polymer serves as electron donors in the CNT/polymer composite [25].

Ultracapacitors (supercapacitors or electrochemical capacitors) are the next generation electric energy storage devices. Conventional capacitors use dielectric materials to separate positive and negative electrodes, while ultracapacitors store electrical charges at an electrode-electrolyte interface as shown in Figure 1.4. When charging, the positive cations in the electrolyte are attracted to the negative electrode, and the negative anions to the positive electrode. Both negative and positive ions in the electrolyte accumulate at the electrode surface to compensate for the electronic charge. Hence, electrical energy is stored inside the electrochemical double layer (the Helmholtz layer) at the electrode-electrolyte interface.

The double layer thickness is usually determined by the electrolyte concentration and the ion size. In concentrated electrolytes it varies between 5 and 10 angstroms [40]. The double layer capacitance for an electrode with smooth surface and concentrated electrolyte is typically in the range of a few uF/cm^2, compared to a few nF/cm^2 for conventional dielectric capacitors, and can be estimated by the following equation [40]:

$$C = \varepsilon_o \varepsilon_r A / d \quad \text{.....1.2}$$

where ε_o, ε_r, d, and A are the permittivity of free space, dielectric constant of the electrolyte, thickness of the double layer, and effective surface area of the electrode, respectively. According to the equation, the capacitance is proportional to the electrode surface area. Therefore, a higher capacitance can be obtained by making electrodes from porous materials with very large effective surface area.

In recent years both MWCNTs and SWCNTs have been studied for supercapacitor applications. Higher capacitance can be obtained by making electrode from nanostructured CNT with extremely large effective surface area.

If a single electrode made of carbon has a surface area of 1000 m^2/g and a double layer capacitance of 10 uF/cm^2, then the specific capacitance would be 100 F/g. An ultracapacitor with two identical electrodes made of the same material should have a specific capacitance of 50 F/g ($1/C=1/C_1 + 1/C_2$). Therefore, reported capacitances need to specify their geometry, either single-electrode or a two-electrode.

The maximum of energy stored in an ultracapacitor is calculated by:

$$W = 1/2(CV_0^2) \quad \text{.....1.3}$$

If the cell voltage V_0 is 1V (typical for aqueous electrolyte), the specific energy stored would be 25 kJ/kg. When an organic electrolyte is used, the cell voltage will be increased to 2.3V and the specific energy will be 66.1 kJ/kg. Although organic electrolytes can achieve higher cell voltage, the specific resistance is 20~50 times higher than that of aqueous electrolytes. The increased resistance of electrolyte affects the equivalent distributed resistance of the porous layer thus reducing the maximum obtainable power, which is determined by the following [40]:

$$P = V^2/4R \quad \text{.....1.4}$$

where R is the total equivalent series resistance (ESR). However, estimation of R of a cell, including the contribution of ion diffusion in the pores and the effects of current transient in the electrodes, is not simple. Nevertheless, a first approximation for the resistance can be written as [40]:

$$R = (2/3)t(r/A) \quad \text{.....1.5}$$

where t is the electrode thickness, and r is the resistivity (Ohm-cm) of the electrolyte.

The relationship for the energy density (Wh/kg) can be expressed as [40]:

$$Wh/kg = (1/8)(F/g)(V^2/3.6) \quad \text{.....1.6}$$

where F/g is the specific capacitance of the electrode material and V is the cell voltage dependent primarily on the electrolyte used in the device.

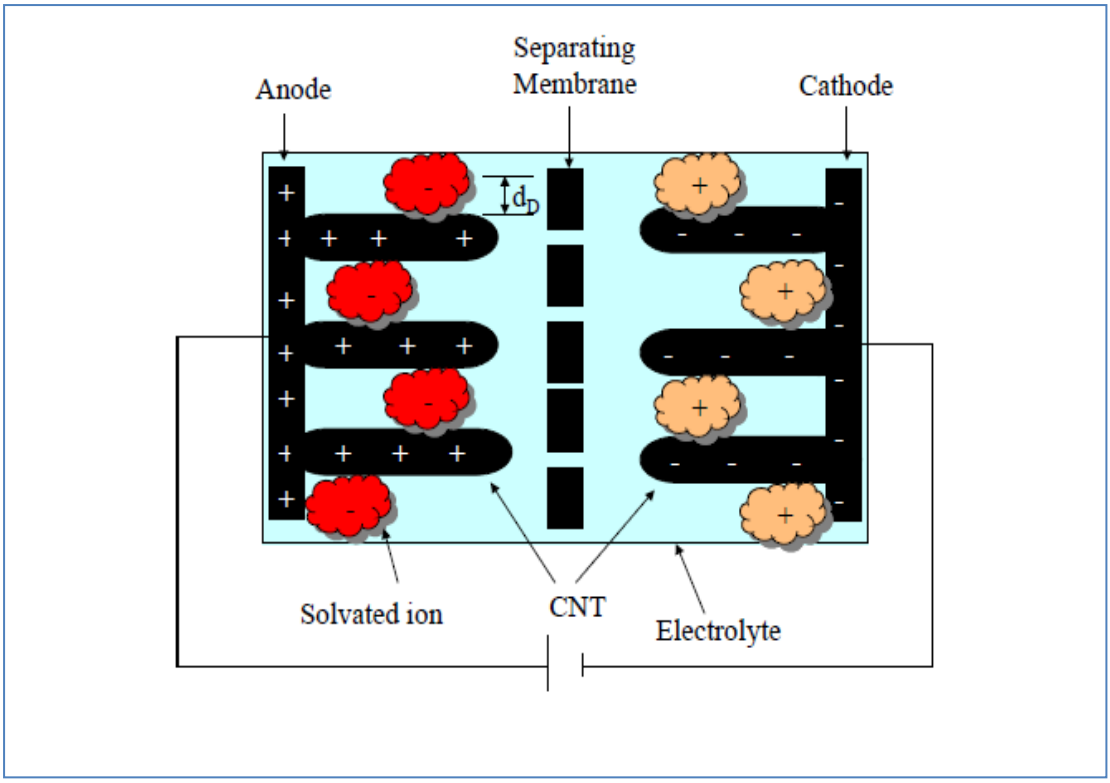

Figure 1.4 General schematic of electrochemical double layer capacitor

Objective of the research

This section describes my research objective of using vertically aligned CNTs as electrode to improve the performance of ultracapacitors. The content of this study is limited to multi-walled carbon nanotubes (MWCNT) grown by hot filament chemical vapor deposition (HFCVD). This research is mainly focused on:

- Selective growth of CNTs using cobalt (Co) catalysts on Ti buffer layer coated n^+ Si wafers.
- Studying the change in CNTs structure by changing gas mixture and growth parameters.
- Fabrication and synthesis of CNTs electrode

- Characterization of the fabricated CNTs electrode
- Characterization of CNT thin films with scanning electron microscope (SEM)
- The effect of hydrogen plasma treatment on CNTs electrode
- The effect of chemical treatments on CNTs electrode
- Electrochemical characterization of CNTs electrode for ultracapacitor applications

Organization of the thesis

The thesis consists of five chapters and three appendices:

- Chapter 1 gives an introduction on structures and properties of carbon nanotubes and carbon nanotubes based electrochemical supercapacitors. The objective of this research is also indicated.
- Chapter II describes the synthesis and characterization of CNTs under different growing conditions, including SEM analysis. In addition, summarizing charts for CNT grown under different conditions are included.
- Chapter III contains the study of electrochemical characterization of CNTs based electrode.
- Chapter IV provides summary and conclusion of the studies described in chapters II and III.
- Chapter V provides recommendations for future research of this work.

CHAPTER II

FABRICATION AND SYNTHESIS OF CNTs

Introduction

This chapter provides the synthesis and characterization of CNTs under different growing conditions, including SEM analysis. In addition, summarizing charts for CNT grown under different conditions are included.

Since the discovered of carbon nanotubes by Iijima in 1991, there have been a variety of techniques developed for the synthesis of CNT. The three most common techniques for producing high quality CNTs include electric arc discharge [41], laser ablation [41], and chemical vapor deposition (CVD) [41]. However, both the arc discharge and laser ablation techniques are quiet limited to volume of samples in comparison to the size of the carbon source. The equipment requirements and large amount of energy consumed by these methods make them unsuitable for laboratory research.

Chemical vapor deposition (CVD) has become the preferred commercial techniques for manufacturing carbon nanotubes. Chemical vapor deposition is a chemical process for producing high performance and high purity solid materials. Enormous research activities have been focused on the control of selective deposition and orientation of CNT by CVD synthesis using various gas sources [5], different substrates [5], and different catalysts [5]. Hot filament chemical vapor deposition (HFCVD) [42] was successfully used to grow multi-walled vertically aligned CNTs.. HFCVD of CNT uses carbon precursor gases such as methane, ethylene, acetylene, ammonia, carbon monoxide or ethanol. The synthesis process usually involves high

temperature decomposition of hydrocarbons (in hydrogen environment) over the catalyst, which is pre-deposited on the silicon substrate. In addition, the capability to control the size, shape, and alignment of CNTs on different substrate surfaces with HFCVD is well documented [41]. In this research, the influence of processing parameters such as buffer layer thickness, catalyst thickness, gases flow rates/compositions, growth temperature, pretreatment time, and growth time on the alignment and morphologies of the synthesized CNT were studied systematically.

Substrate preparation prior to CNT growth is an important factor in CNT synthesis. Generally, substrate preparation includes substrate cleaning process and deposition of catalytic metal layer. In this study magnetron sputtering was used for deposition of buffer layer and metal catalyst on Si substrates.

Previous to the magnetron sputtering, the silicon samples have to be carefully cleaned by chemical etching. A buffer oxide etch (BOE) is commonly used to etch windows in n^+ type silicon wafer [43]. The BOE is a mixture of a buffering agent, such as ammonium fluoride (NH_4F) [44], and hydrofluoric acid (HF) [44] in deionized water and at specific concentrations. Silicon etching is performed by immersing the silicon substrates in BOE solution.

To grow CNT by catalytic method, the substrate has to be deposited with catalyst. A common way of depositing metallic catalyst on silicon substrate is by using magnetron sputtering, which can also be used to deposit a broad range of materials such as Ti, Ni, Al, and Co. Sputtering is achieved by bombarding a target with energetic ions, typically Ar^+ [43]. In this study, magnetron sputtering was used to coat Ti (as a buffer layer) and Co (as a catalyst) onto the silicon surface.

Experiment

Two sets of experiments were performed to examine the role of different process parameters on the growth of CNTs. The synthesis parameters are shown in Table 2. For all set of experiments, a HFCVD-BM 1000 system equipped with a filament cartridge including four tungsten wires was used to grow CNTs. In addition, BOE and magnetron sputtering were used for sample preparations.

First of all, highly conductive n^{++} silicon substrates with resistivity of 0.0035 Ω-cm and 2.5 cm x 1.5 cm in size were used for growing CNT. The BOE solution was prepared in 300 mL glass beaker. The substrates were immersed in BOE solution to remove the native oxidize from the silicon surface for 5 minutes. Then, they were rinsed with methanol and deionized water and dried by Ar gas. In magnetron sputter deposition, the Cressington 308R DC magnetron sputtering system equipped with thickness monitor and power supply was used in this study. The silicon substrates were first coated with a thin layer (~15nm thick) of titanium (Ti) followed by a thin layer (~5nm thick) of cobalt (Co), under a vacuum of ~$5x10^{-5}$ Torr [5]. The thin Ti layer serves as a buffer preventing the possible reaction of Si with Co to form cobalt silicate.

The first experiment consists of samples A1-A5 is divided into five groups having all samples with the same thickness of buffer-catalyst layer (Ti/Co 15nm/5nm). The second experiment consists of samples B1-B5 is also divided into five groups having all samples with the same thickness of buffer-catalyst (Ti/Co 15nm/5nm). Samples from each group of experiments were then subjected to different processing parameters as described in Table 2.

Table 2: Specific details of the synthesis parameters used to grow CNTs. The parameters include buffer/catalyst thickness, temperature (T), pressure (P), flow rates, pretreatment time, and growth time

Exp	no	Catalyst	Temperature-Pressure Flow rates					Pretreatment time	Growth time
		Ti/Co	T	P	H_2	CH_4	NH_3	H_2/NH_3	CH_4
		nm	^0C	Torr	Sccm	Sccm	Sccm	Minutes	Minutes
1	A1	15/5	700	15	75	25	75	40/5	2
	A2	15/5	700	15	75	25	75	40/5	4
	A4	15/5	700	15	75	25	75	40/5	6
	A5	15/5	700	15	75	25	75	40/5	8
	A6	15/5	700	15	75	25	75	40/5	10
2	B1	15/5	700	15	75	25	100	40/5	2
	B2	15/5	700	15	75	25	100	40/5	4
	B3	15/5	700	15	75	25	100	40/5	6
	B4	15/5	700	15	75	25	100	40/5	8
	B5	15/5	700	15	75	25	100	40/5	10

After the substrates were coated with a thin layer of titanium and cobalt they were loaded into the HFCVD system for growth of CNTs, per the processing parameters described in Table 2. After loading the sample, the HFCVD system was pumped down to a base pressure of ~ 0.2 Torr, with the predetermined hydrogen gas flow rate. After getting this base pressure, the substrate temperature was increased to 700 ^{0}C, gradually. The samples from all the groups were subject to same working temperature (~700 ^{0}C). For both the first and second experiment, hydrogen (H_2), methane (CH_4), and ammonia (NH_3) gases were used to grow vertically aligned CNTs. The pretreatment run for 40 min with H_2 and then H_2/ NH_3 gases were fed into the reaction chamber of HFCVD for 5 min. At this time the temperature of the filament was increased to 1900 ^{0}C. After the pretreatment step, the methane (CH_4) is then introduced immediately to initiate the synthesis of CNTs. A combination of H_2/ NH_3/CH_4 with 75:75:25 (sccm) flow ratios, and in another run a combination of H_2/ NH_3/CH_4 with 75:100:25 (sccm) flow ratios were fed into the reaction chamber. The reaction pressure and temperature of the filament for the growth were ~15 torr and 2000 ^{0}C, respectively. The time taken for the pretreatment was 45 minutes. The growth time varies from 2 to 10 min.

Samples A1-A5, in the first experiment, were grown with CNT in the HFCVD system by applying H_2/NH_3/CH_4 gas mixture (75:75:25 sccm) for different growth time (2, 4, 6, 8, and 10 min) at 700 ^{0}C substrate temperature. Likewise, samples B1-B5, in the second experiment, were grown with CNT under the same processing conditions as the first experiment except the gas mixture. The H_2/NH_3/CH_4 gas mixture in this case is 75:100:25 sccm.

Experimental Results and Discussion

The catalyst particle sizes and distributions, and the morphology of CNT such as average tube diameter, tube height, tube density of all the samples were observed and determined with a Hitachi S4200 scanning electron microscope (SEM). In addition, the role of ammonia has been investigated both in the pretreatment phase and growth of CNT phase. During the growth phase for both experiments 1 and 2, ammonia might generate atomic hydrogen species providing etching effects for the amorphous carbon generated during the CNT synthesis. It is a well-known fact that ammonia is a more effective generator of atomic hydrogen than H_2 as the addition of ammonia to a H_2/CH_4 mixture. The hydrogen was also found to play an important role in this experiment. The hydrogen increased the catalyst activity on the surface of CNT and it changed the hydrocarbon (CH_4) percentage to reduce amorphous carbon particles on top of CNTs. Consequently, ammonia and hydrogen are believed to be essential to the growth of CNTs, although the reason responsible for the effect of ammonia in CNT growth has not been clearly known yet.

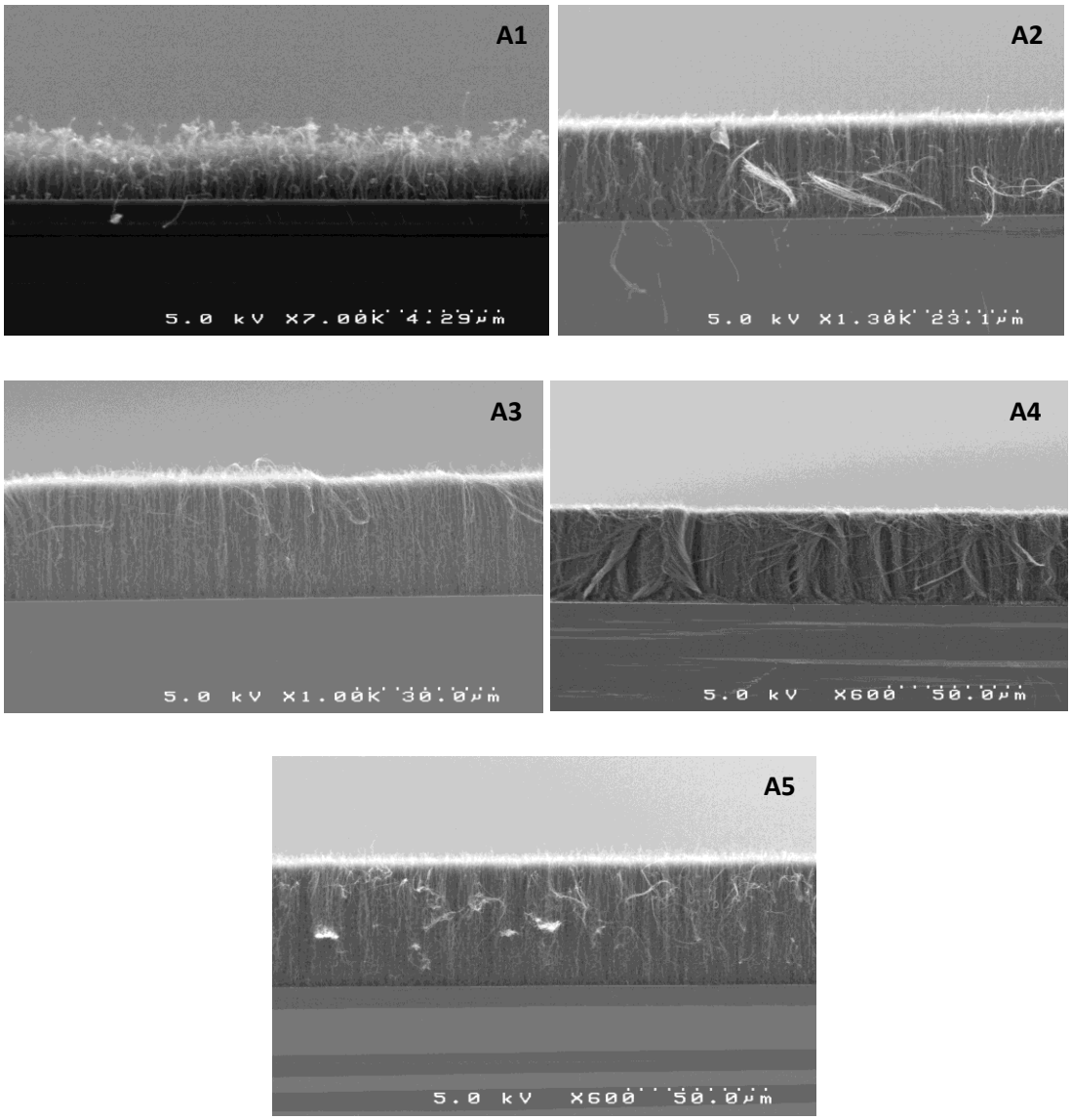

Figure 2.1: SEM cross section images of CNTs with different growth time at ~75 sccm NH_3 parameter. Growth time of CNT, 2 min, 4 min, 6 min, 8 min, and 10 min, respectively.

Five different growth times were applied to CNT synthesis with the intension to evaluate the growth time on fabricated CNT physical parameters. As shown in Figure 2.1, the as-grown CNTs are seemly well vertically aligned and contain few carbon nanoparticles.

According to the SEM images, it is clear that sample A1 has more amorphous carbon compared to the rest. Samples A2, A3, A4, and A5 have better physical alignment and less amorphous carbon. Overall in experiment 1, sample A5 has the best alignment with height ~50μm. Moreover, we have also observed from other experiments (not shown here) that the substrate temperature also plays an important role in CNT synthesis. It affected CNT height and alignment due to catalytic decomposition of hydrocarbon such as methane, and ethane.

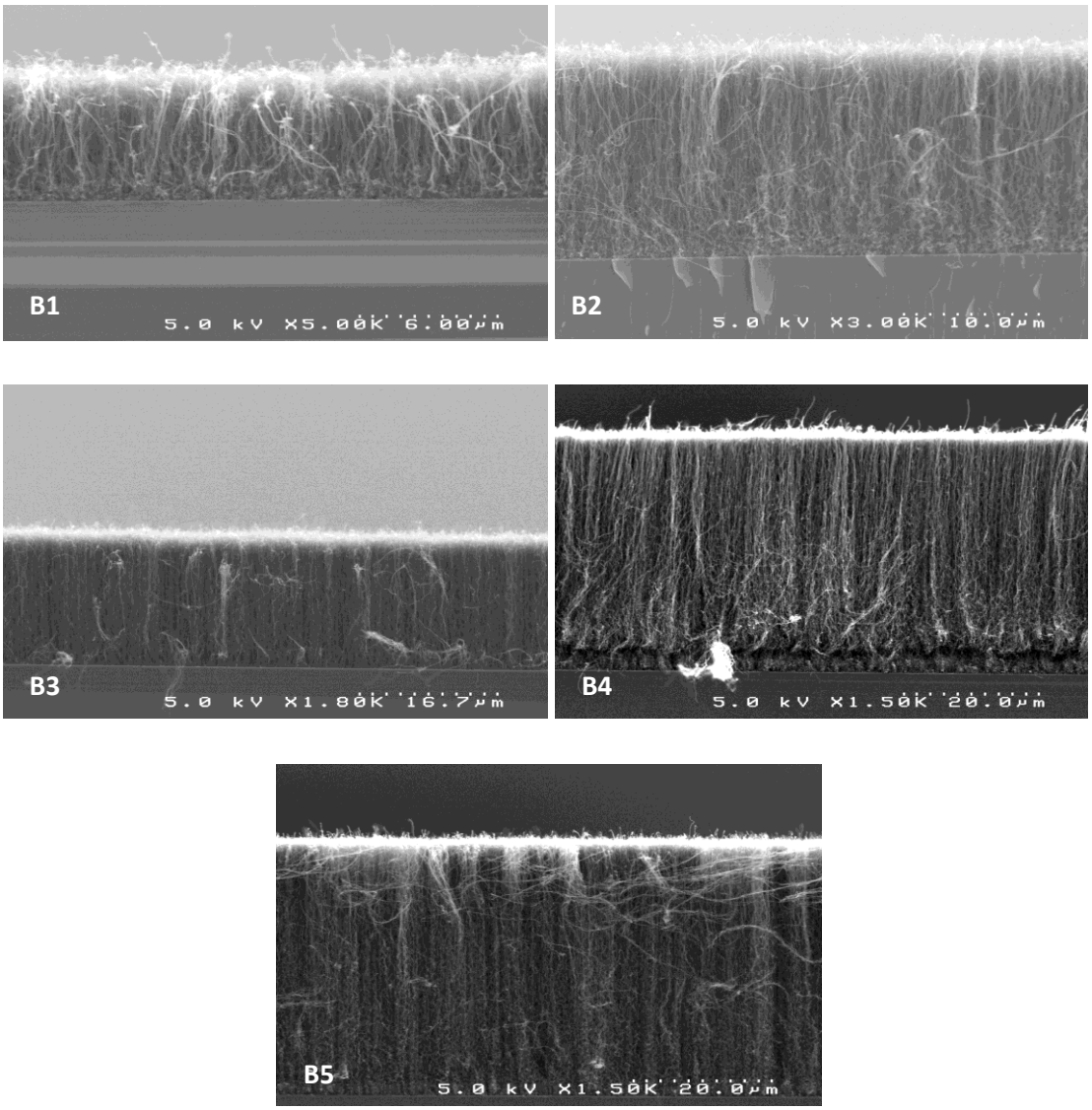

Figure 2.2: SEM cross section images of CNTs with different growth time at ~100 sccm NH_3 parameter. Growth time of CNT, 2 min, 4 min, 6 min, 8 min, and 10 min, respectively.

As shown in Figure 2.2, the CNTs are found to be much more aligned and almost no amorphous carbon on the top. However, the CNTs are shorter in length compare to first experiment except sample B1. For sample B1, it seems that two minutes growth time is not enough for obtaining well aligned CNTs. It has been shown that longer growth time gave advantage for achieving well-aligned and taller CNTs. Overall in experiment 2, sample B5 has the best alignment with height ~42μm. In addition, amorphous carbon contamination has been decreased from sample B5 to B1.

The comparison of two samples from the corresponding experiments 1 and 2, it is clear that sample B1 has better alignment and taller CNTs compared to sample A1. For sample A2 and B2, interesting result has been observed. Although sample A2 and sample B2 have different ammonia flow rate, the CNTs are almost same height ~17μm. By comparing sample A3 and B3, sample A3 has ~30μm height and sample B3 has ~19μm height. This significant change can be explained by experimental conditions. The comparison of samples A4 and B4, sample A4 has ~40 μm height and sample B4 has also ~40 μm. By comparing sample A5 and B5, sample A5 has ~50μm height and sample B5 has ~42 μm height. It has been shown that role of ammonia in CNT growth was not completely clear. It is shown that in Figure 2.3.

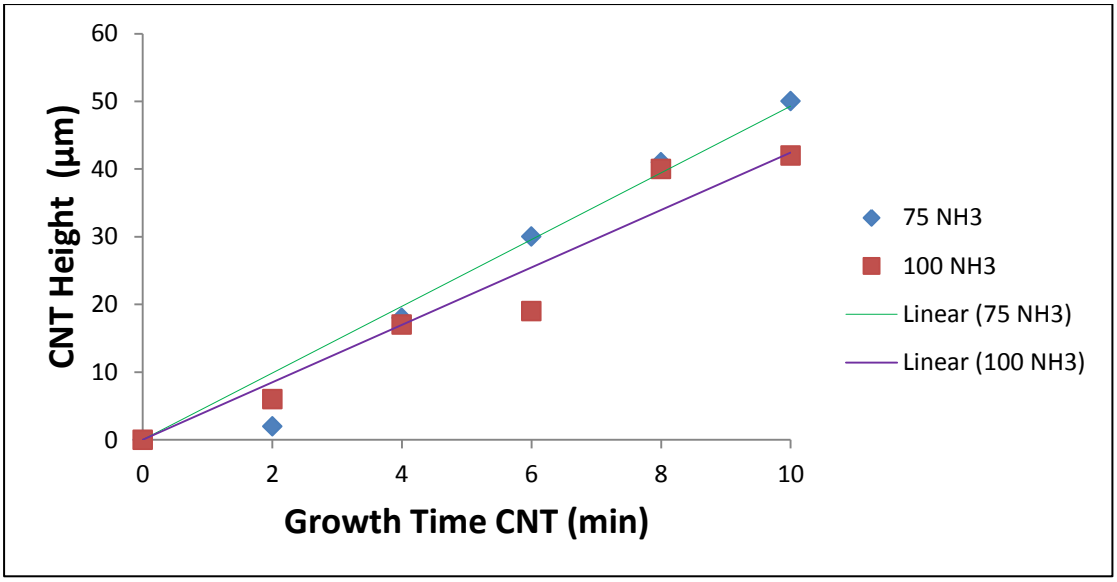

Figure 2.3: CNT height (µm) versus Growth time CNT (min)

Throughout the experiment the role of ammonia on the carbon nanotube growth and the effect of growth time on CNTs were investigated. Moreover, growth characteristics of carbon nanotubes changed from spaghetti-like to vertically aligned when the growth condition was switched from low to high ammonia ratio. Furthermore, the length of carbon nanotubes changed from ~2 µm to ~50 µm when the growth time was switched from short to long time. The details of the synthesis parameters are shown in table 2.

CHAPTER III

ELECTROCHEMICAL CHARACTERIZATION OF CNTs BASED ELECTRODE

Introduction

In previous chapter, we have reported the growth of vertical-aligned CNTs by controlling the ammonia (NH_3) flow rate and growth time, using hot filament chemical vapor deposition (HFCVD). This chapter introduces electrochemical characterization of CNTs based electrode. The first part of this chapter presents the voltammetric measurements of the CNTs based electrodes and their corresponding capacitance measurements. The second part of this chapter describes the effects of chemical treatments on the CNTs based electrode, including electrochemical impedance analysis and galvanostatic charge/discharge test.

The electrochemical supercapacitor behavior of CNTs based electrode has been characterized by cyclic voltammetry, impedance analysis, and charging-discharging test in KCl electrolyte. Cyclic voltammetry, also known as sweep reversal method, is the most popular electrochemical characterization method [45] and is a type of potentiodynamic electrochemical measurement [46]. In cyclic voltammetry, the electrode potential ramping (characterized by scan rate (V/s)) is applied between the reference electrode and working electrode. The resulted current is measured between the working electrode and the counter electrode [46] and is plotted as current (I) versus potential (V). Consequently, cyclic voltammetry provides both quantitative and qualitative information of the electrochemical behavior of the working electrode.

The electrochemical analysis was performed in a glass flat cell as shown in Figure 3.1 using the standard three-electrode configuration, namely the working electrode (WE), counter electrode (CE), and reference electrode (RE). In this set up, the potential of the working electrode is followed comparative to reference electrode, nevertheless, the current passes between the working electrode and counter electrode [45]. Experimentally, the reference electrode should be placed closely to the working electrode in order to decrease the solution resistance [45].

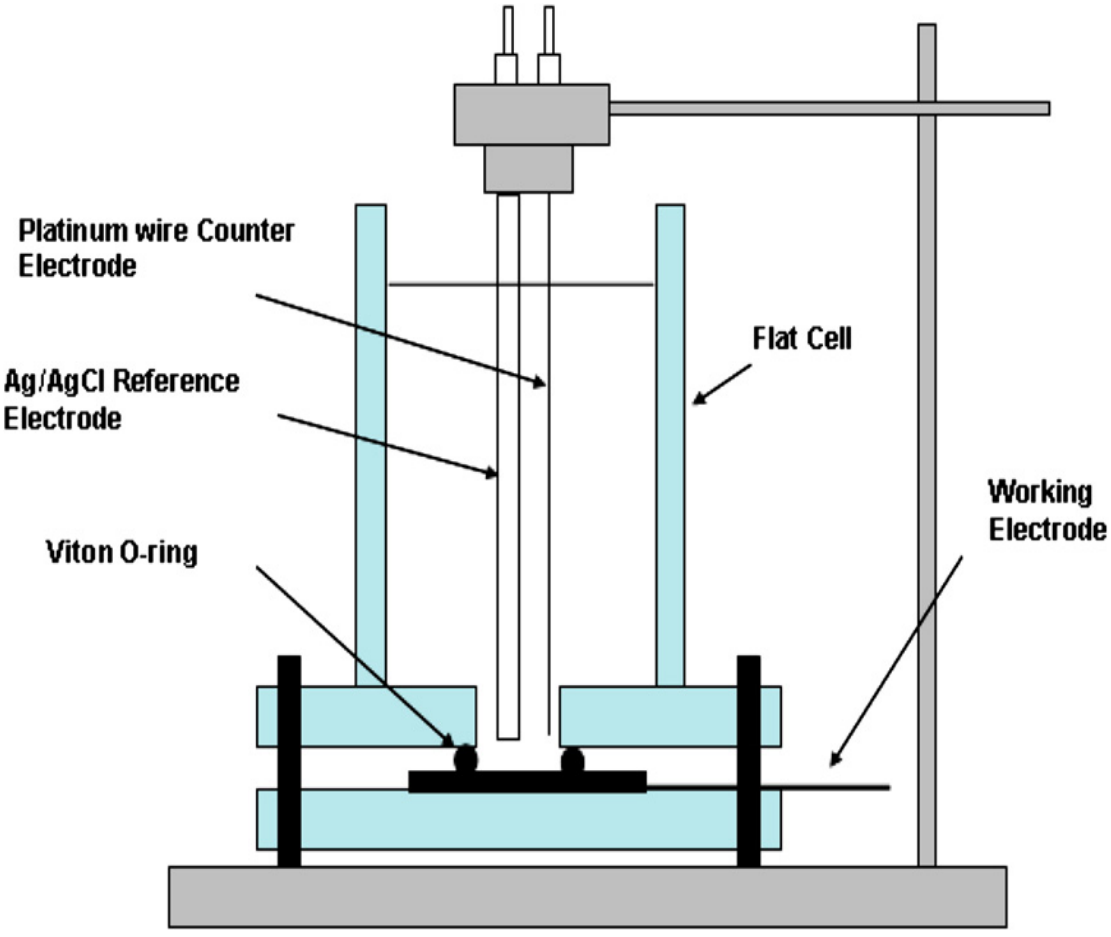

Figure 3.1: Test setup for electrochemical analysis [45].

Experiment

The electrochemical performance of the CNTs based ultracapacitor electrode is determined by voltammetric measurement at room temperature in a standard three-electrode flat cell as shown in Fig 3.1 using Pt wire as the counter electrode and Ag/AgCl as the reference electrode. A 0.1 M KCl aqueous solution was used as the supporting electrolyte.

Electrochemical analysis was performed in a CH 620 instrument using the accompanying software. The scanning voltage range was set between 0 and 1 V. Previous to all experiments, the back side of working electrode substrate was lightly wiped with a cotton applicator soaked with BOE to remove the native oxide and to make good electrical contact with the underlying copper tape [47].

In this experiment, the electrode active test area is defined by the circular O-ring with a radius r.

$$A = \pi r^2 \quad \ldots\ldots\ldots\ldots\ldots\ldots\ldots\ldots\ldots\ldots\ldots\ldots\ldots\ldots\ldots \text{(1)}$$

The electrode active test area for all samples was calculated to be ~ 0.712 cm^2. The capacitance of each sample can be obtained from the cyclic voltammograms per [48]:

$$C = I/[\left(\frac{dv}{dt}\right)A]\ldots\ldots\ldots\ldots\ldots\ldots\ldots\ldots\ldots\ldots\ldots\ldots\ldots.... \text{(2)}$$

where *C* is the electrode capacitance, *I* is the measured capacitive current, *dv/dt* is the scan rate, and *A* is the electrode area.

Experimental Results and Discussion

In this study, seven samples (75 sccm NH_3-4 minutes CNT (A2), 75 sccm NH_3-6 minutes CNT (A3), 75 sccm NH_3-10 minutes CNT (A5), 100 sccm NH_3- 4 minutes CNT (B2), 100 sccm NH_3-6 minutes CNT (B3), 100 sccm NH_3- 8 minutes CNT (B4), and 100 sccm NH_3-10 minutes CNT (B5)) were used for cyclic voltammetry experiment. The potential scan window was set for 0 to 1 V with scan rate varied from 10 to 800 mV/s. Ideal supercapacitor should be able to maintain a rectangular shaped I-V curve over a wide range of scan rate [48].

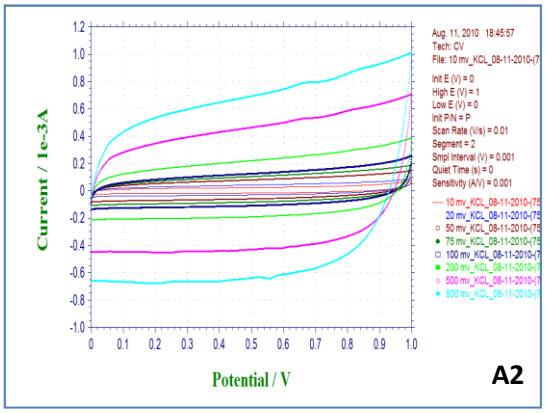

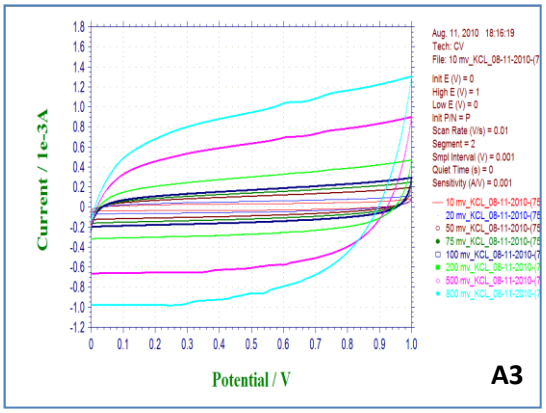

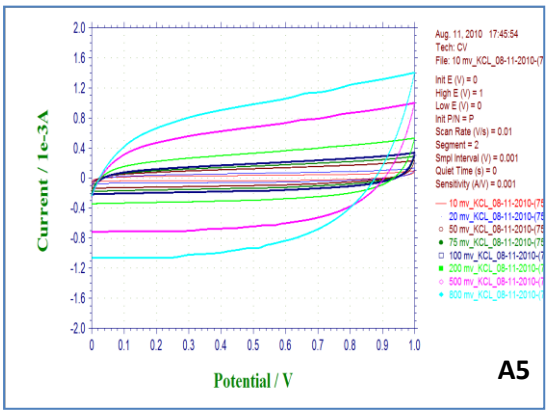

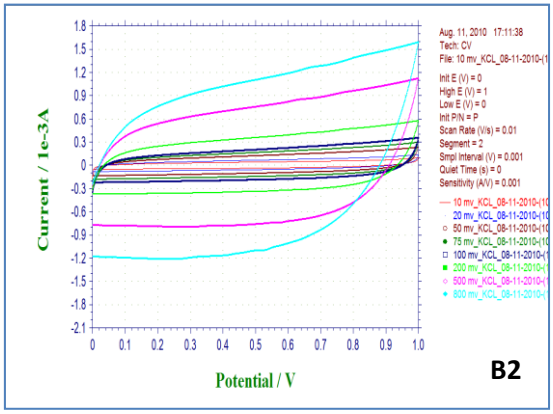

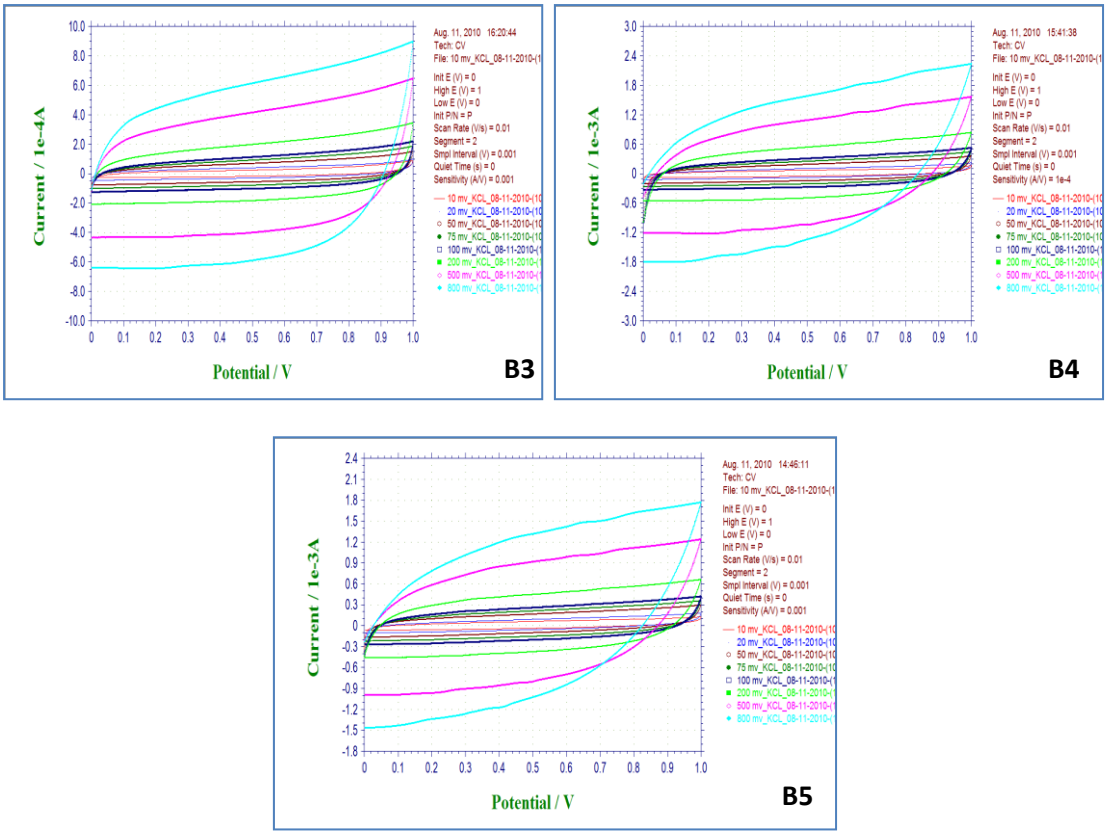

Figure 3.2: Cyclic voltammograms of as-grown CNT electrodes obtained from samples A2, A3, A5, B2, B3, B4, and B5, respectively, at various scan rates.

As shown in Figure 3.2, for all the samples examined, rectangular shaped I-V curves were generally obtained while the scan rate is varied from 10 to 800 mV/s. Sample A2 and B3 have better rectangular shaped I-V curves compared to other samples. The fast charging-discharging behavior can be expected from sample A2 and B3 while having more close a rectangular shaped I-V curve.

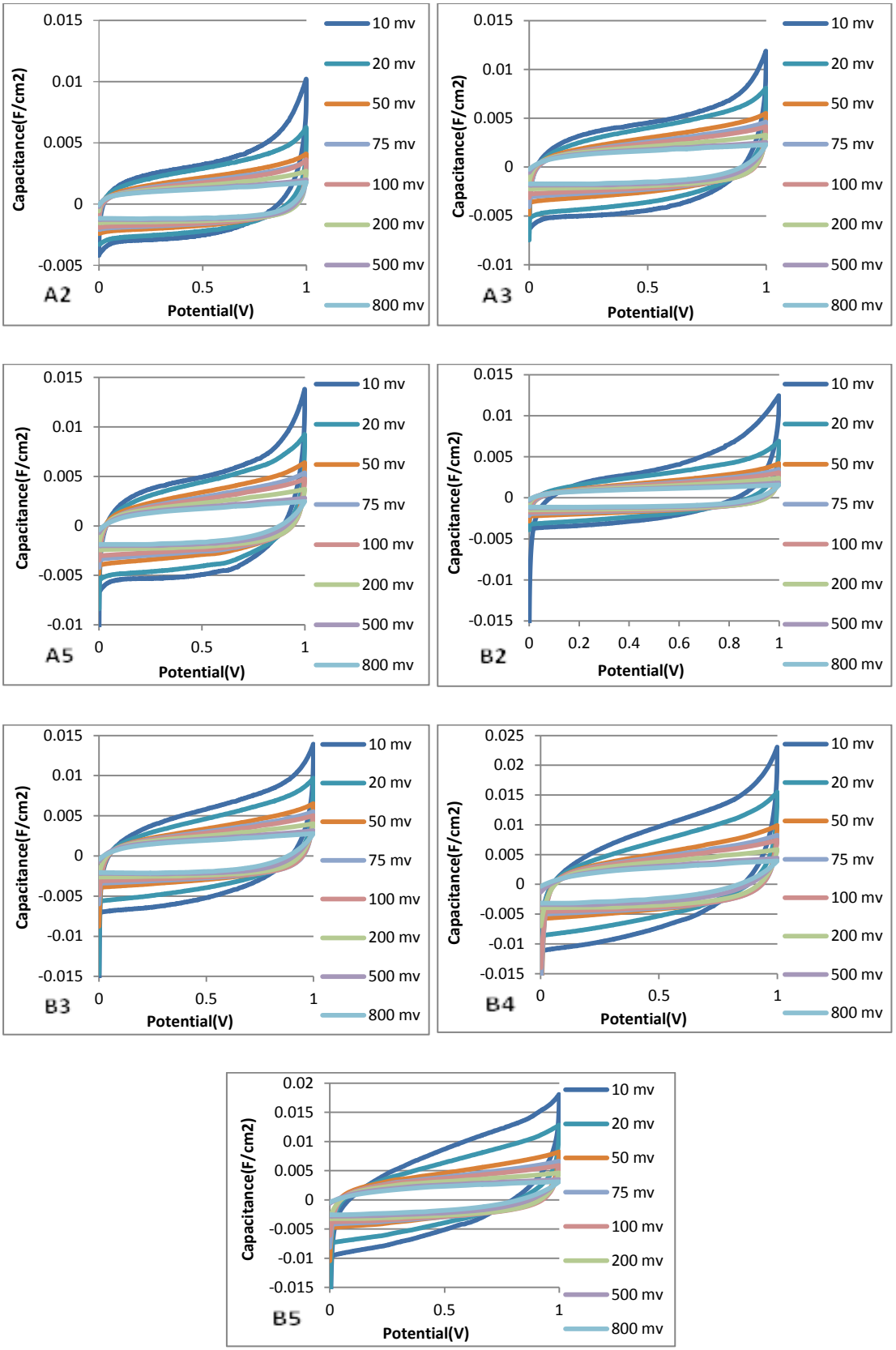

Figure 3.3: Capacitance voltammograms of as-grown CNT electrodes obtained from sample A2, A3, A5, B2, B3, B4, and B5, respectively, at various scan rates.

The corresponding capacitance-voltage plots of all the samples are shown in Figure 3.3. Sample B4 have the highest capacitance value and sample A2 have the lowest capacitance value. As previously discussed, electrode capacitance is dependent on the capacitive current, scan rate, and total effective surface area of the carbon nanotubes. Better tube alignment yields higher density of nanotubes. Higher quantity of CNTs per unit area generates higher capacitance. It is obvious that sample B4 has better vertical aligned CNTs on its structure. In other words, sample B4 has higher density of nanotubes per unit area. Therefore, sample B4 has the highest capacitance compared to other samples.

Figure 3.4 shows electrode capacitance vs. CNTs height for all the samples measured. Generally, for the two groups of samples fabricated using two different NH_3 flow rates, the electrode capacitance increases linearly as the CNTs height increased. Moreover, the figure also shows that higher ammonia flow rate in the as grown CNT samples provided higher electrode capacitance compared to those fabricated with lower ammonia rate. As previously discussed, the role of ammonia on CNTs structural parameters is still not known. Further analysis of the effects of ammonia on the physical and chemical properties of the fabricated CNTs need to be performed in order to understand the observed improvement in electrode capacitance at higher ammonia flow rate.

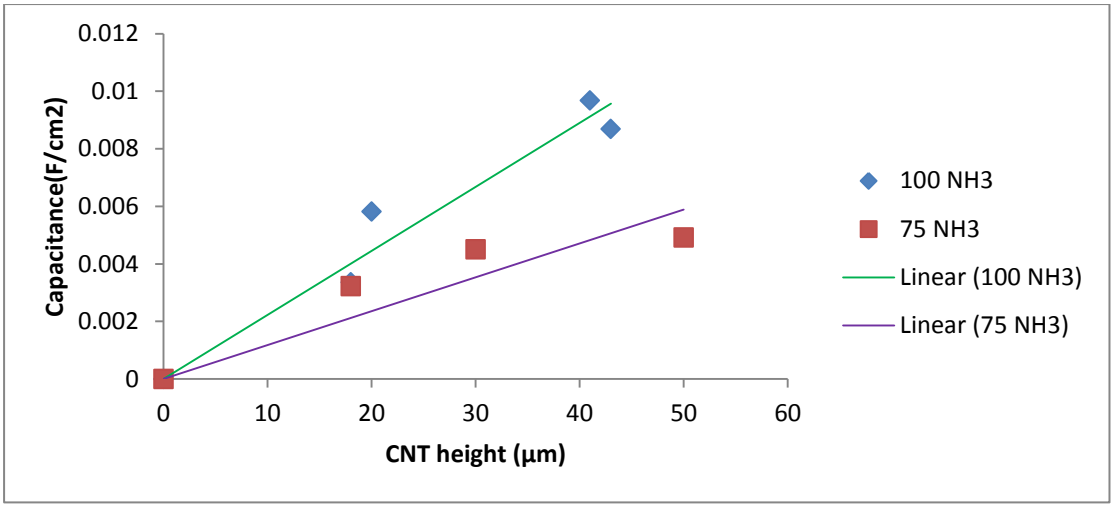

Figure 3.4: Capacitance (F/cm^2) versus CNT height (µm)

As shown in Figure 3.5. The electrode capacitances were decreased exponentially with scan rate in this experiment. According to equation 2, the electrode capacitance depends on relationship between the current and scan rate. Relationship between the current and scan rate becomes particularly important in the study of electrode capacitance. According to equation 3, the current is proportional to square root of the scan rate. If the scan rate is altered the current response also changes.

$$I_p = 2.69*10^5*n^{3/2} * A*D^{1/2}*C*v^{1/2} \text{.....(3)}$$

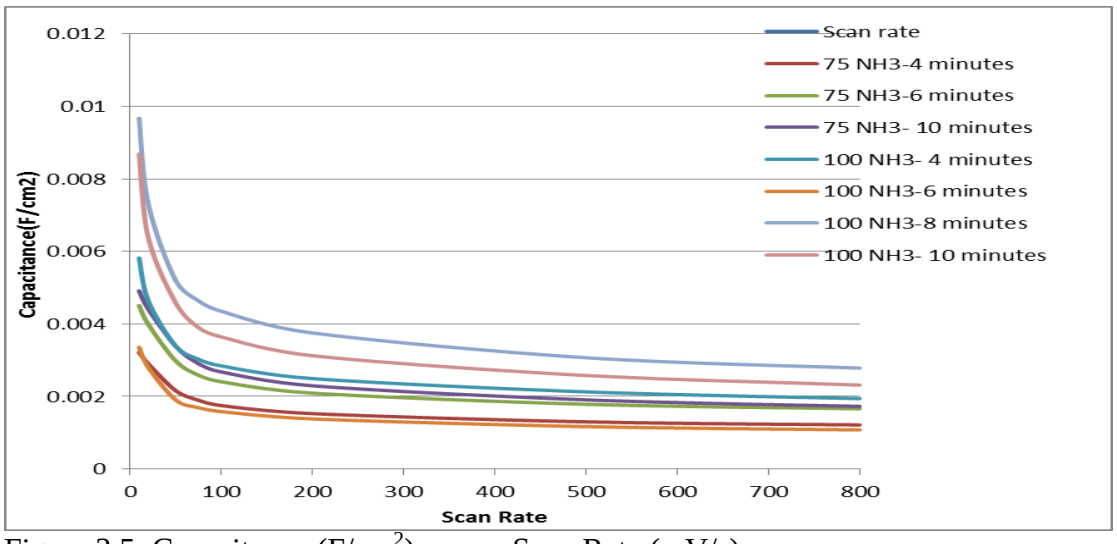

Figure 3.5: Capacitance (F/cm^2) versus Scan Rate (mV/s)

Chemical Treatments of CNTs Based Electrode, Electrochemical Impedance Analysis, and Galvanostatic Charge-Discharge Test

This section describes the effects of post synthesis treatments on the electrochemical performance of CNTs based electrodes. These include polyvinyl alcohol (PVA) treatment, H_2O_2 (hydrogen peroxide) treatment, H_2 (hydrogen) plasma treatment, and their effects on charge and discharge characteristic, and impedance (Z) characteristic of the electrodes. The goal is to explore the possibility of using post synthesis treatment method to enhance CNTs supercapacitor performance.

Surface functionality of CNTs can be modified via oxidation with different liquid-phase oxidizing agents such as hydrogen peroxide [37], nitric acid (HNO_3) [24], ammonium persulphate $(NH_4)_2S_2O_8$ [37], potassium permanganate ($KMnO_4$) [50], and polyvinyl alcohol [51]. The oxidation of CNTs can also be made with other methods such as oxygen plasma treatment [52]. During oxidation treatment, functional oxygen groups such as carbonyl, carboxylic, phenol [53], lactol [53], and hydroxyl are formed on the surface of carbon nanotubes [50].

Our first approach on CNT surface modification is to treat as grown hydrophobic CNTs with polyvinyl alcohol to increase the electrode capacitance. The molecular structure of polyvinyl alcohol is shown in Figure 4.1.

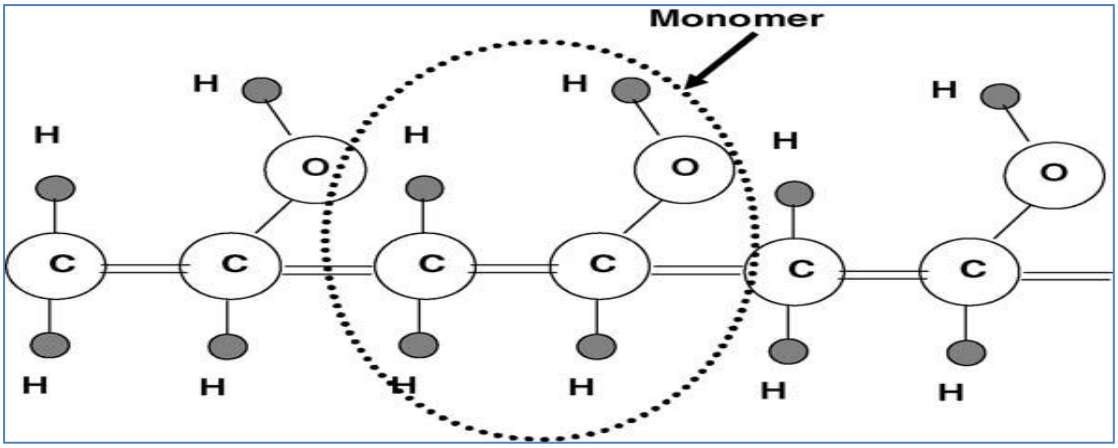

Figure 4.1: Polyvinyl alcohol structure. Every carbon has OH^- group in the chain [51].

Recent studies by Kozlov [51] have shown that PVA can change the hydrophobic surface of CNTs into hydrophilic surface. It is known that as grown CNTs have hydrophobic surface, so having hydrophilic CNT surface with polyvinyl alcohol are of interest for several applications.

Our second approach on CNTs surface modification is to investigate the effects of hydrogen peroxide treatment on carbon nanotubes. Hydrogen peroxide, also known as mild oxidant [50], is widely used in the etching [54], and purification [54] of CNTs in recent studies. Even though hydrogen peroxide is not very strong oxidized agent as the nitric acid, it has advantage compared to other oxidized agents. It can be used under different conditions that other oxidized agent cannot infer [50]. Hydrogen peroxide treatment was used to generate functional oxygen groups on the surface of CNTs similar to polyvinyl treatment.

Our third approach on CNTs surface modification is to investigate the effects of hydrogen plasma treatment on carbon nanotubes. The goal of this work is to make CNTs surface as pure as possible by hydrogen plasma etching. The hydrogen plasma treatment is actually very similar to hydrogen peroxide treatment.

They remove amorphous carbon and metal catalyst impurities on surface of CNTs [55]. It is well known that as grown CNTs surface contains metal catalyst nanoparticles and amorphous carbon [56].

The electrochemical impedance spectroscopy (EIS) measurements were performed for all treated samples, in frequency ranging from 1Hz to 1 MHz [57]. The Nyguist complex plane impedance is generally plotted, $Z^{//}$ (real) versus $Z^{/}$ (imaginary), which may include a small semicircle at high frequency due to bulk RC response and vertical spike at low frequency due to the nature capacitor behavior [58].

The galvanostatic charge/discharge test was also performed to evaluate the CNTs electrodes capacitive behavior [58] at a constant current for all treated samples. It is well known that galvonastatic charge/discharge test gives most accurate results for carbon nanotube based supercapacitors. The cell capacitance can be calculated from the charge/discharge curves [59].

Experiment

In this study, three samples (75 sccm NH_3-6 minutes CNT (A3), 75 sccm NH_3-10 minutes CNT (A5), and 100 sccm- NH_3-6 minutes CNT (B3)) were used to determine the effect of surface treatments on CNTs electrode. Sample A3 was used for hydrogen peroxide treatment, sample A5 was used for hydrogen plasma treatment, and sample B3 was used for polyvinyl alcohol treatment.

For the case of polyvinyl alcohol treatment, polyvinyl alcohol powder, laboratory grade (%87 hydrolyzed-100 g), was used. Polyvinyl alcohol solution was prepared by dissolving PVA powder in deionized water (~18.2 MΩ). Then the PVA solution was placed on the hot plate for 1 hour at 90 ^{0}C with stirring speed 850 rpm.

The sample B3 was placed in the middle of the glass flat cell as shown Figure 3.1 with the CNTs exposed/immersed in the PVA solution for 4 hours, 16 hours, 30 hours, and 60 hours, separately. After each experiment the substrate was rinsed with deionized water and dried in oven at 100 ^{0}C for 1 hour.

To investigate the effect of polyvinyl alcohol treatment on CNTs electrode, cyclic voltammetry was performed in a CH 620 workstation using the related software. Then, impedance measurements were performed using a.c impedance technique provided by the workstation, and galvanostatic charge/discharge was investigated using chronopotentiometry technique in same station.

For the case of hydrogen peroxide treatment, we first prepare hydrogen peroxide solution by mixing 10 ml hydrogen peroxide with 50 ml deionized water in a beaker. After hydrogen peroxide solution was prepared, the sample A3 was placed in the middle of flat cell shown in Figure 3.1 with the CNTs exposed/immersed in hydrogen peroxide solution at 65 ^{0}C for 24 hours. After that hydrogen peroxide solution was poured away from flat cell. Lastly, cyclic voltammetry, impedance measurements, galvanostatic charge/discharge test was performed in a 0.1 M KCl aqueous solution.

For the case of hydrogen plasma treatment, sample A5 was placed in ASTEX 1.5 kW microwave plasma enhanced chemical vapor deposition (MPCVD) system operated at substrate temperature of 650 ^{0}C, hydrogen pressure of 20 Torr, and plasma power of ~ 400 W for 120 sec. Then, SEM pictures were taken to examine the CNT surface morphology due to plasma treatment. It was observed that hydrogen plasma treatment for 120 sec was enough to remove amorphous carbon and metal nanoparticles from the CNTs surface.

Experimental Results and Discussion

As shown in Figure 4.2, after PVA treatment the cyclic voltammetry (CV) curves exhibited close to rectangular shape at scan rates of 10 mV/s, 20 mV/s, 50 mV/s, 75 mV/s, 100 mV/s, and 200 mV/s; whereas at a scan rate of 500 mV/s and 800 mV/s, the capacitance due to the effects of IR drop was observed.

It can be seen from the I-V curves that PVA treatment for 16 hours was enough to functionalize carbon nanotubes surface. It is believed that the saturation point for PVA treatment on CNTs was approximately 16 hours. Therefore, there were no significant changes in I-V curves of CNTs for the 30 hours and 60 hours PVA treatments.

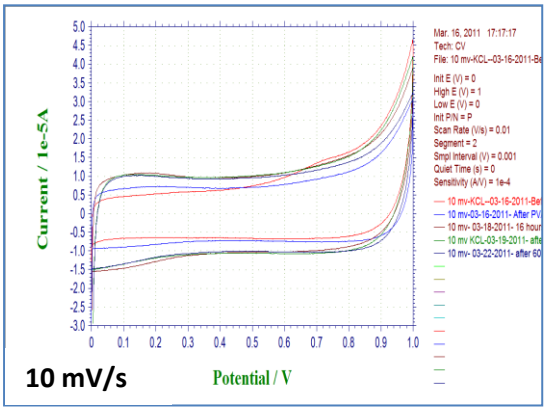

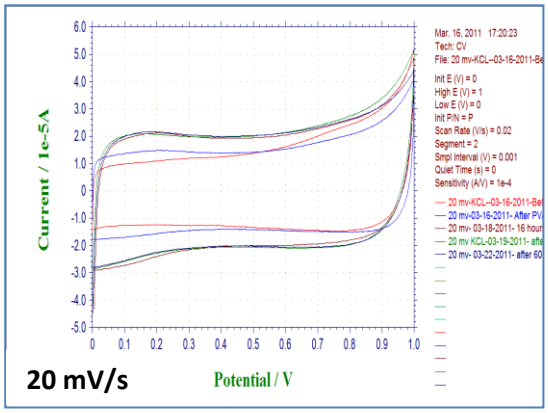

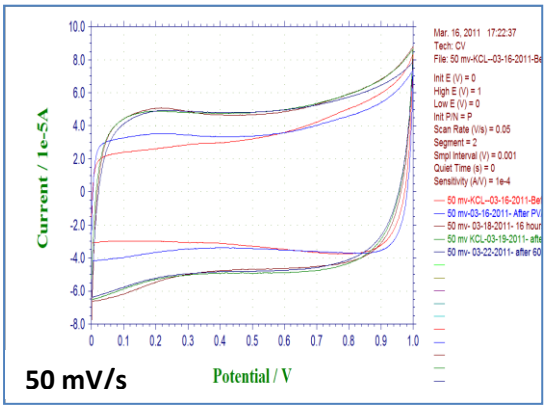

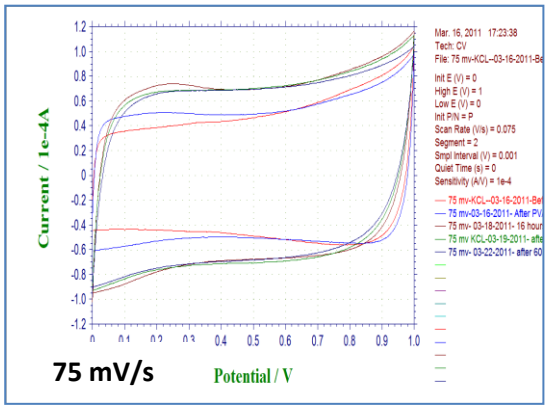

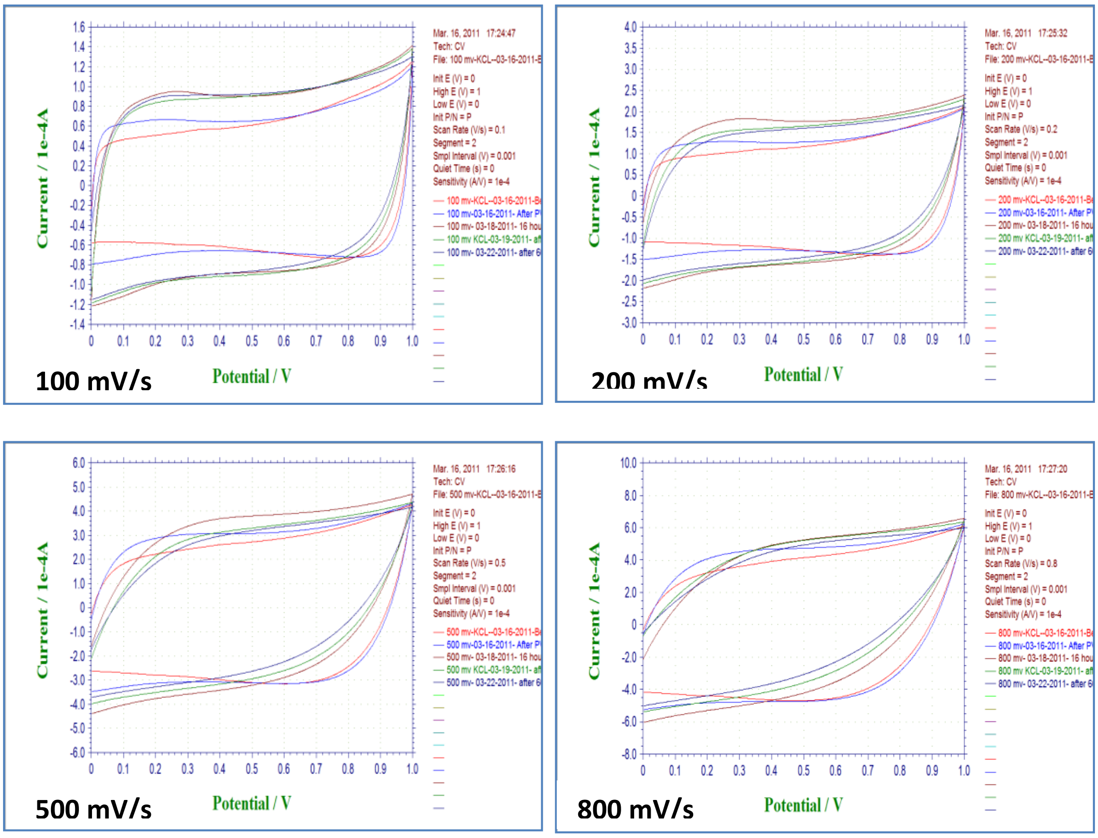

Figure 4.2: Cyclic voltammograms for sample B3 after different PVA treatment times (4, 16, 30, and 60 hours) at various scan rates (10, 20, 50, 75, 100, 200, 500, and 800 mV/s).

Impedance measurement was performed after cyclic voltammetry. It is well known that impedance is one of the most important parameter for capacitors. The impedance (Z) as a function of frequency can be calculated as follow:

$$Z\ (\Omega) = R + J\ X_C \quad \ldots\ldots\ldots\ldots\ldots\ldots\ldots\ldots\ldots\ldots\ldots\ldots \ (4)$$

$$Z\ (\Omega) = R + J\ (-1/\ \omega\ C) \quad \ldots\ldots\ldots\ldots\ldots\ldots\ldots\ldots\ldots \ (5)$$

$$Z\ (\Omega) = R + J\ (-1/\ 2\ \pi\ f\ C) \quad \ldots\ldots\ldots\ldots\ldots\ldots\ldots\ldots \ (6)$$

where Z (Ω) is electrical impedance, R is resistance, J is the imaginary unit, X_C is the capacitive reactance, ω is angular frequency, and f is frequency.

Impedance plots can be divided into high and low frequency regions. The plot of Z_{Im} vs Z_{Re} should be linear at low frequency regions and should be a small semicircle at high frequency regions. The impedance decreases with the frequency until it self-resonant frequency is reached. Above resonance, the impedance becomes inductive and increases with frequency. It is easy to understand the relationship between capacitance and impedance from equation 5. While the capacitance (C) and frequency (f) increase, the impedance (Z) will decrease gradually. The impedance of the CNTs electrodes at various frequencies is shown in Figure 4.3.

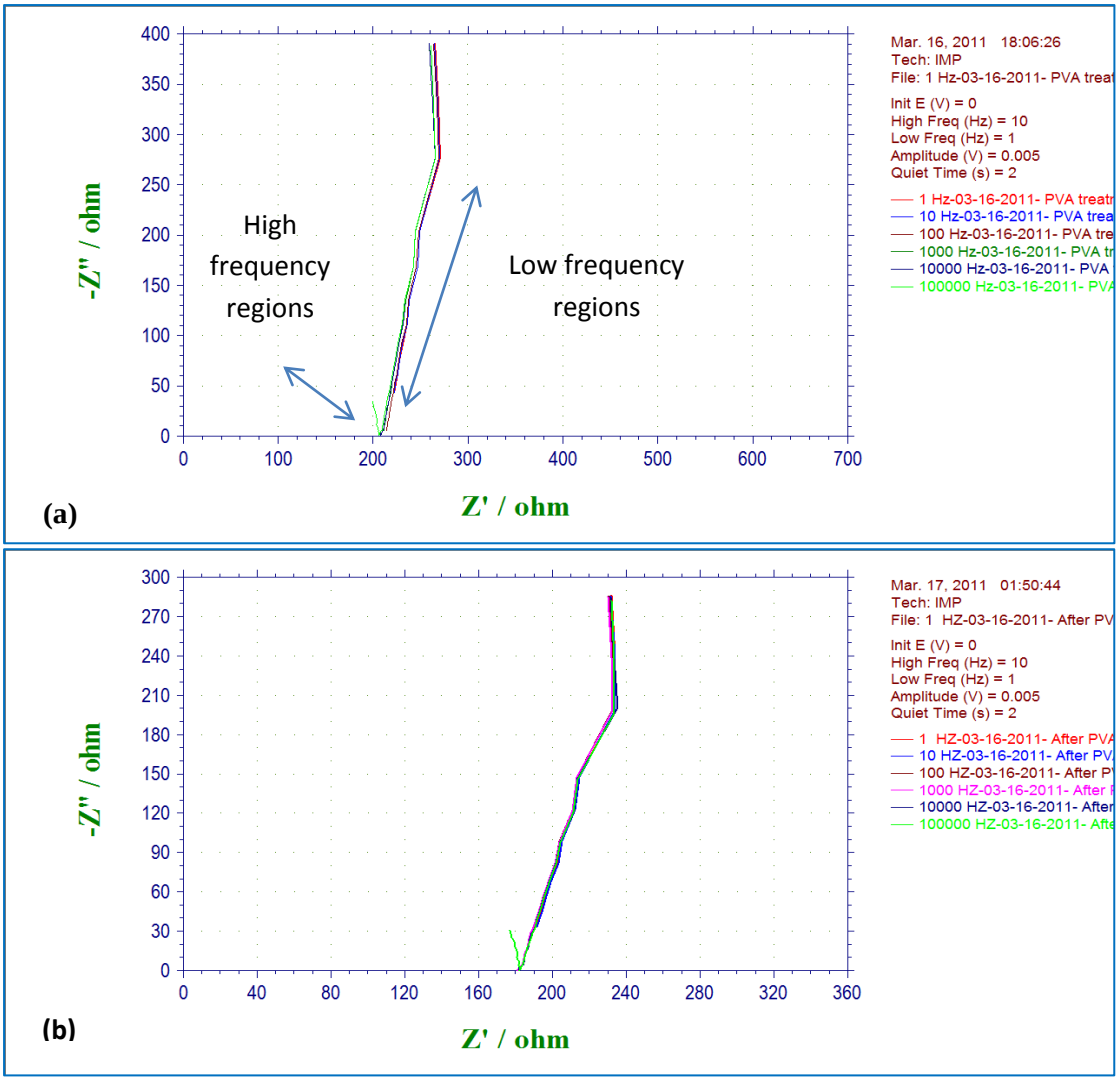

Figure 4.3: Nyquist complex impedance plots ($Z^{'}$ (real) versus $Z^{''}$ (imaginary)), (a) before and (b) after PVA treatments.

As shown in Figure 4.3, the real ($Z^{'}$) part of impedance was used as reference point for impedance calculation. The impedance plot was measured in the frequency ranging from 1Hz to 100kHz. The lowest impedance was achieved at high frequency for before and after PVA treatment.

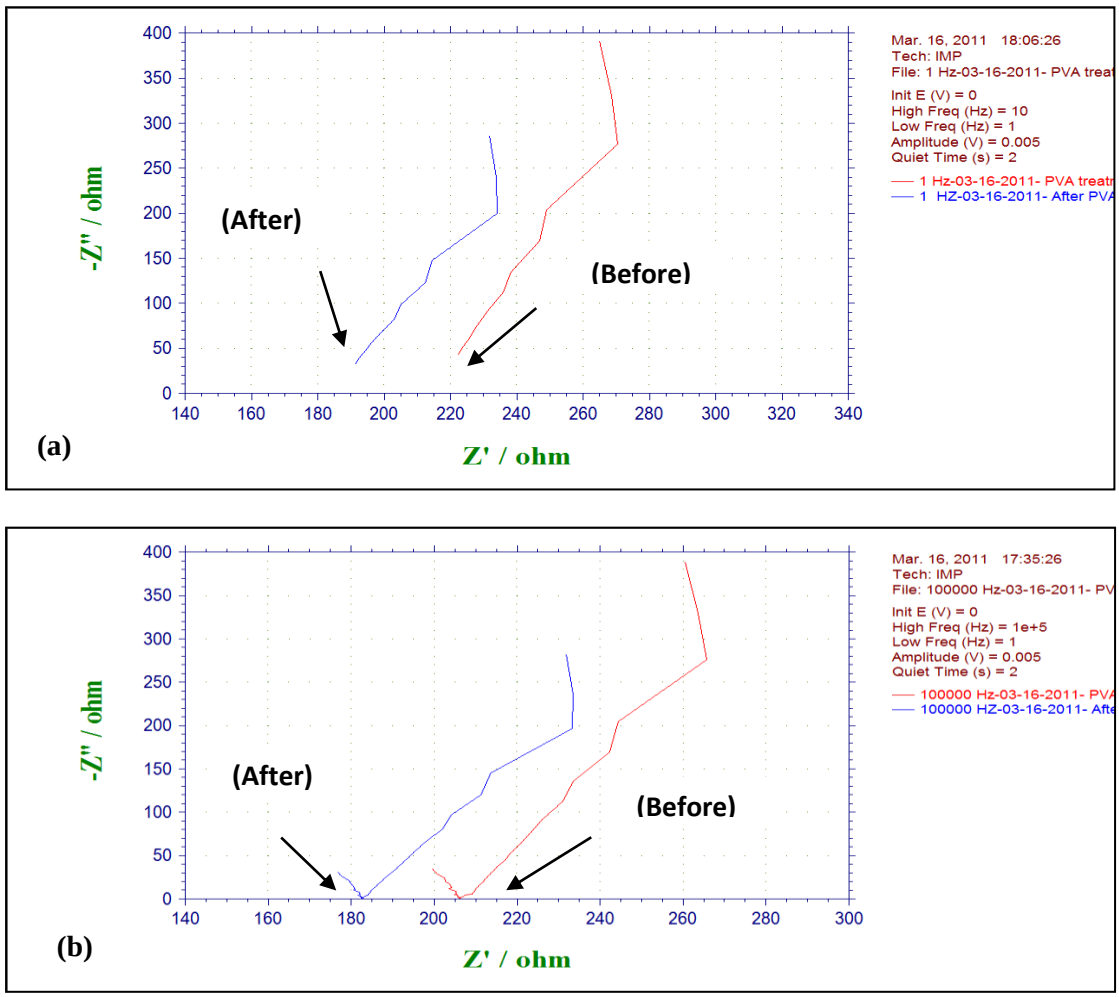

Figure 4.4: Nyquist complex impedance plots at various frequencies (a) 10 Hz (b) 0.1 MHz.

As shown in Figure 4.4, after PVA treatment the impedance was decreased by more than ten percent at a constant frequency. Therefore, the capacitance was increased with decreasing impedance value according to equation 5. The impedance becomes inductive and increases with frequency above resonance at 0.1 MHz.

Galvanostatic charging/discharging tests were performed after impedance measurements. It is well known that charging/discharging behavior is one of the most important parameter for capacitors. Based on the charging/discharging cycle and current, the capacitance can be estimated for each of the electrode sample as follow:

$C = I*t/V$……………………………………………(7)

where I is the charging current, t is the charging time for each cycle, and V is the cell voltage (set at 0.85V for all samples in this case).

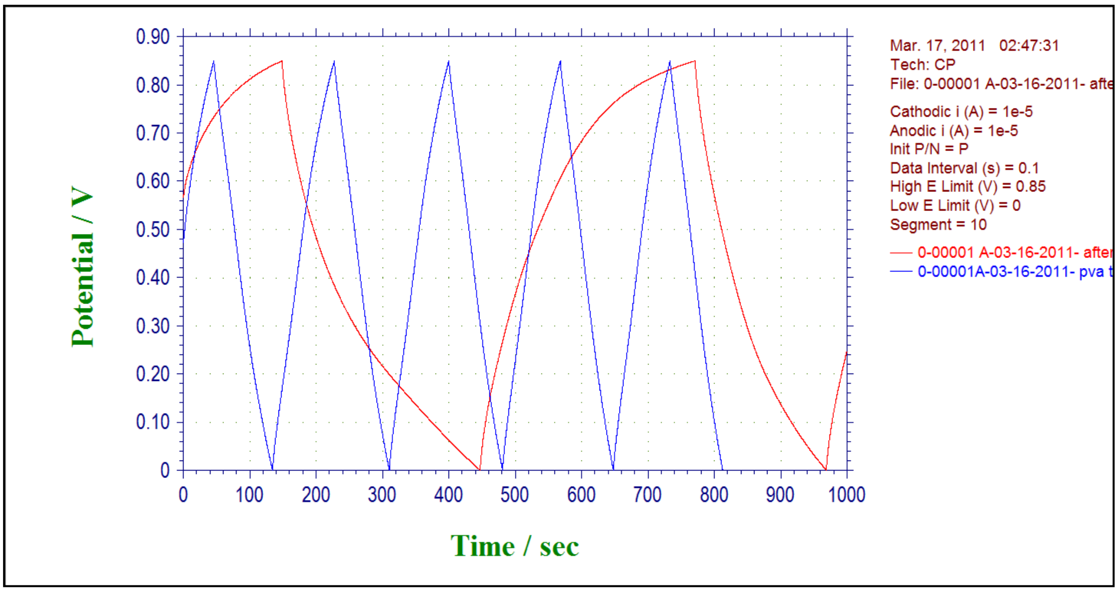

Figure 4.5: Galvanostatic charge/discharge cycles at 10 µA cm^{-2}.

To examine the cyclic stability and further quantify the capacitance, galvanostatic charging/discharging tests have been performed on the above samples and the results are shown in Figure 4.5. The red and the blue lines correspond to PVA treated and untreated CNT sample, respectively, at charging/discharging current of 10 µA. In figure 4.5, it can be seen that the charging time of each cycle for the blue and red lines was 86.6s and 264.2s, respectively. And the calculated capacitance was 1018.82µF and 3108.23µF, accordingly. The PVA treated CNT sample has capacitance three times the untreated CNT sample.

Consequently, it inferred that the CNT surfaces were transformed from nature hydrophobic to hydrophilic with PVA treatment. Therefore, PVA treatment is a useful method for enhancing the capacitance of CNTs.

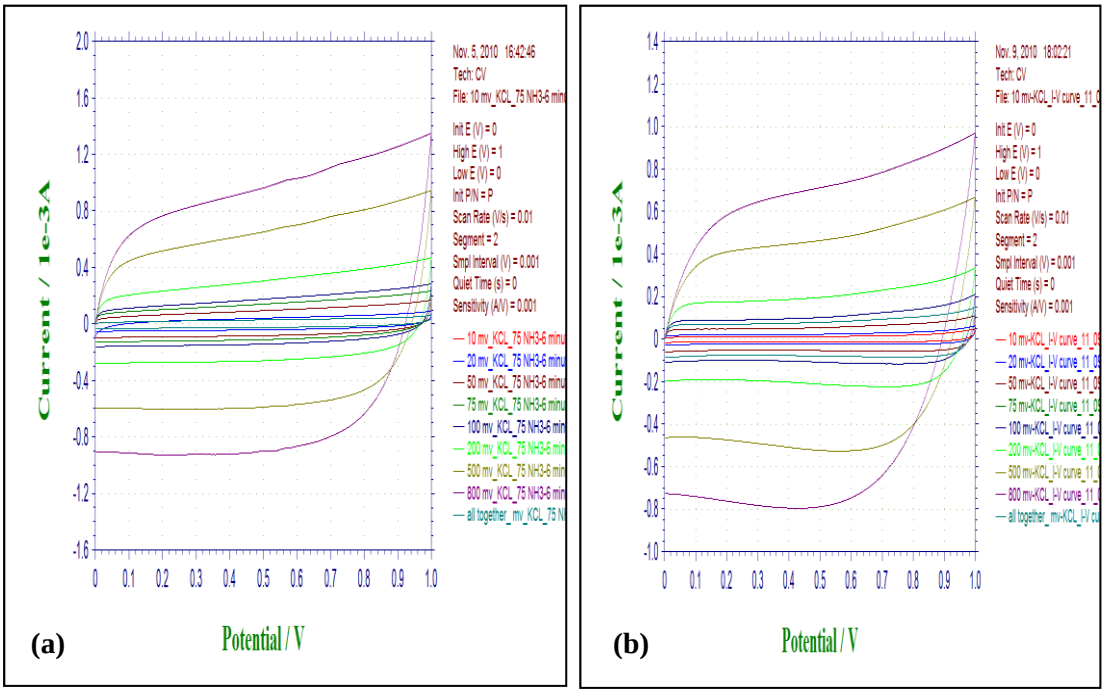

Figure 4.6: Cyclic voltammetry for sample A3 at various scan rates (10, 20, 50, 75, 100, 200, 500, and 800 mV/s), (a) before and (b) after hydrogen peroxide treatments.

Figure 4.6 shows the cyclic voltammetry curves (CV) of CNTs electrode before and after hydrogen peroxide treatment, at scan rates of 10 mV/s, 20 mV/s, 50 mV/s, 75 mV/s, 100 mV/s, 200 mV/s, 500 mV/s, and 800 mV/s. As previously discussed, hydrogen peroxide can make either oxidative damage to the CNT structure or produce new oxygenated groups on CNTs surface.

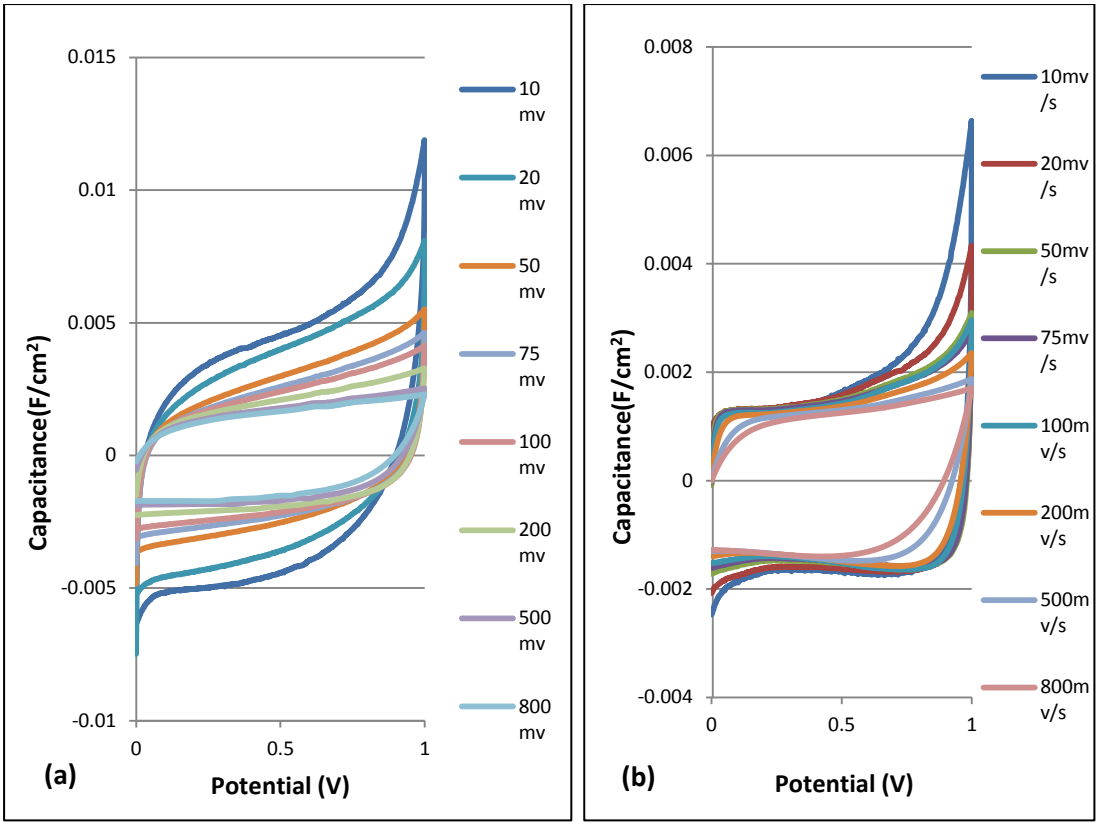

Figure 4.7: C-V curves for hydrogen treatment (a) before (b) after, at various scan rates (10, 20, 50, 75, 100, 200, 500, and 800 mV/s).

As shown in Figure 4.7, the C-V curve maintained the rectangular shape while the scan rate was varied from 10 to 800 mV/s. However, it is readily seen that capacitance value decreased after hydrogen peroxide treatment. Oxidative damage with hydrogen peroxide treatment could be the reason of this behavior.

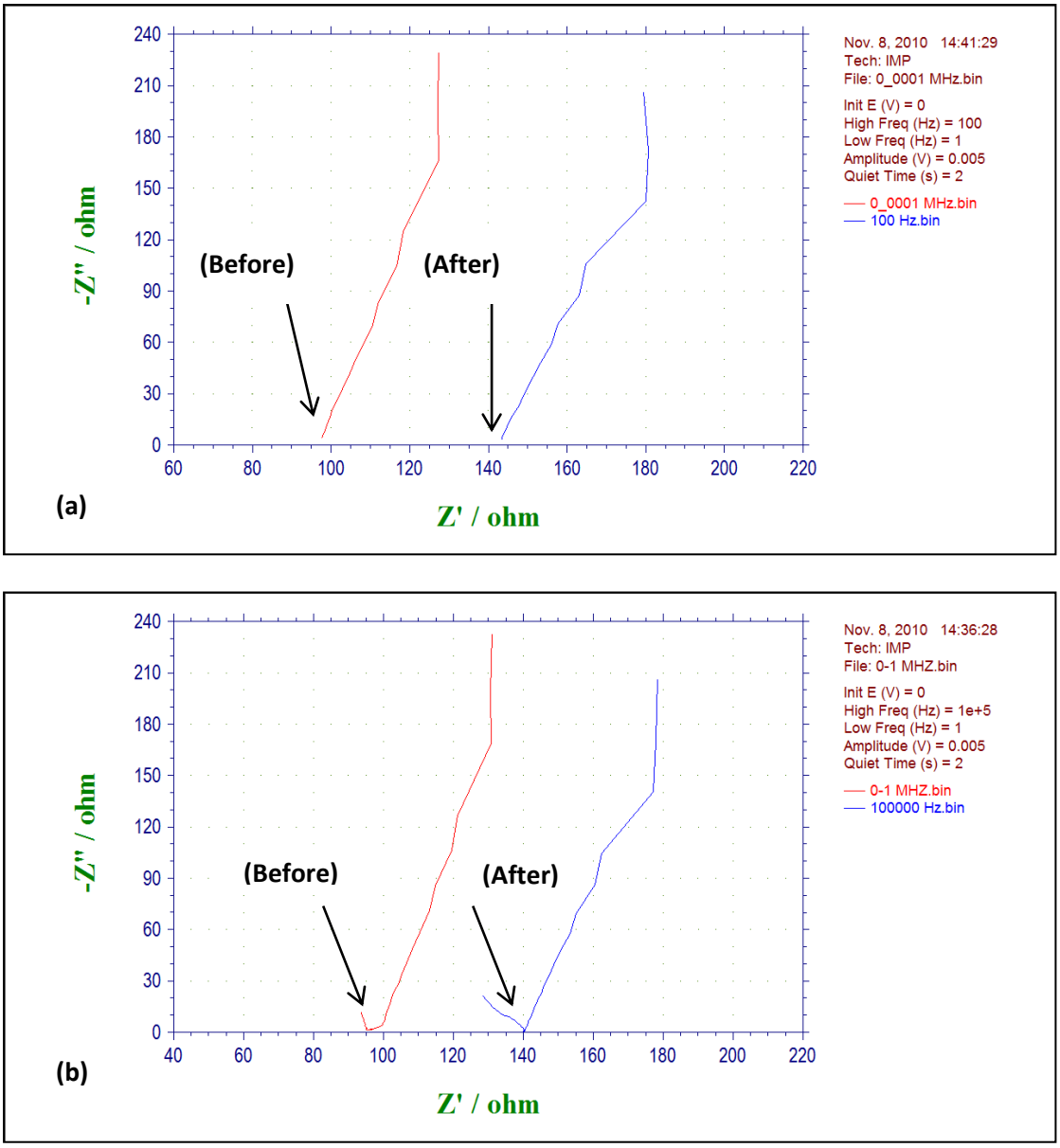

Figure 4.8: Nyquist complex impedance plots at various frequencies (a) 100 Hz (b) 0.1 MHz.

As shown in Figure 4.8, after hydrogen peroxide treatment, the impedance increased prominently and capacitance decreased at a constant frequency according to equation 4. It is well known the impedance increases gradually with decreasing capacitance.

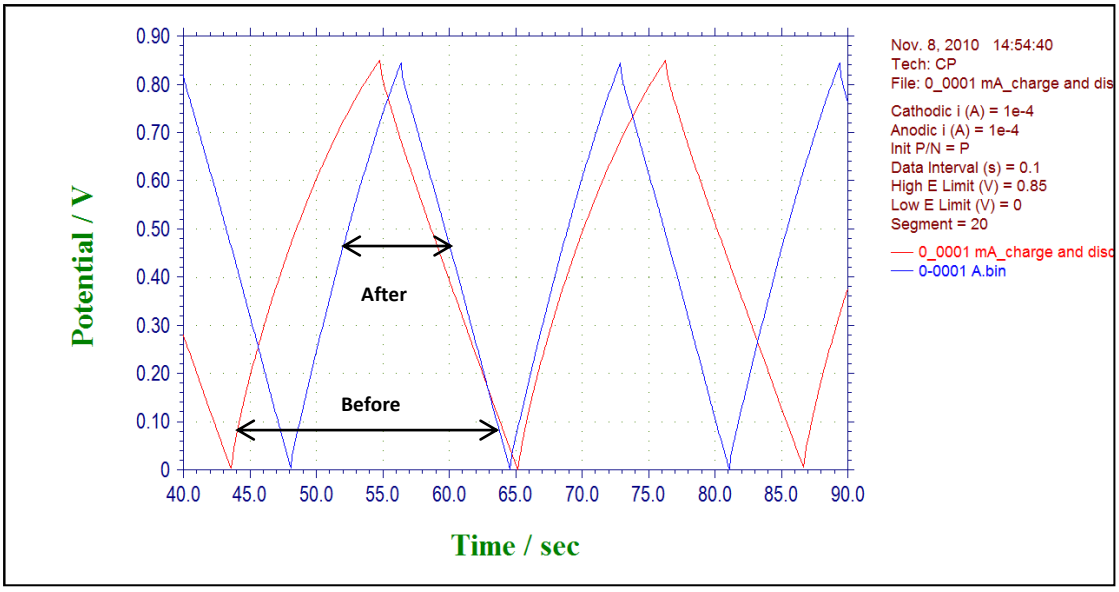

Figure 4.9: Galvanostatic charge/discharge cycles at current density of 100 μA cm^{-2}.

As shown in Figure 4.9, the voltage increases and decreases almost linearly with time between 0 and 0.85 V. The red and blue lines correspond to hydrogen peroxide treated and untreated CNT samples, respectively, under the same charging-discharging current of 100 μA. The charging time of each cycle for the above samples was found to be 21.73s and 16.4s, respectively. The calculated capacitance was 2556.47μF and 1929.41μF, accordingly. It was clearly seen that the capacitance was decreased after hydrogen peroxide treatment. These results illustrated that hydrogen peroxide treatment is not useful for functionalization of CNTs surface.

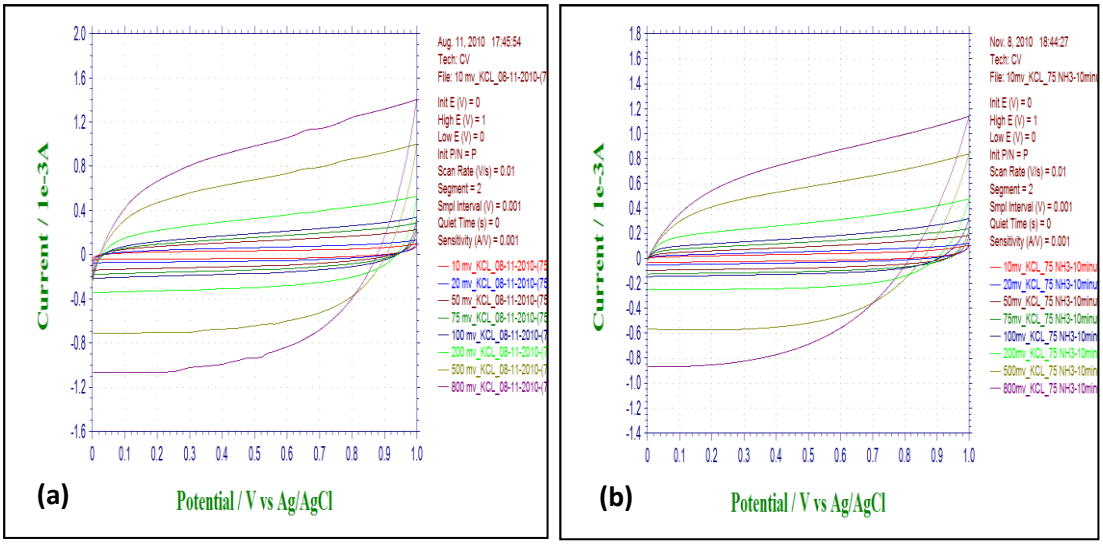

Figure 4.10: Cyclic voltammetry for sample A5 at various scan rates (10, 20, 50, 75, 100, 200, 500, and 800 mV/s), (a) Before hydrogen plasma treatment (b) after hydrogen plasma treatment.

Finally, hydrogen plasma treatment was investigated. I-V curves show that there is no significant change after treatment as shown in figure 4.10.

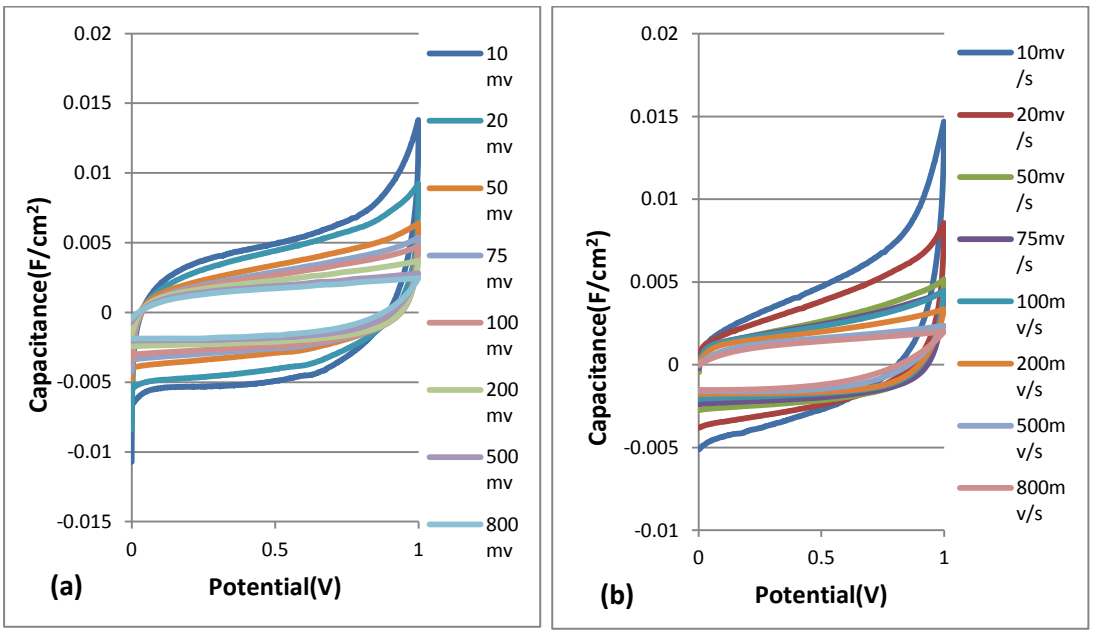

Figure 4.11: C-V curves for hydrogen plasma treatment (a) before (b) after, at various scan rates (10, 20, 50, 75, 100, 200, 500, and 800 mV/s).

As shown in Figure 4.11, the capacitance curves remained almost the same before and after treatments.

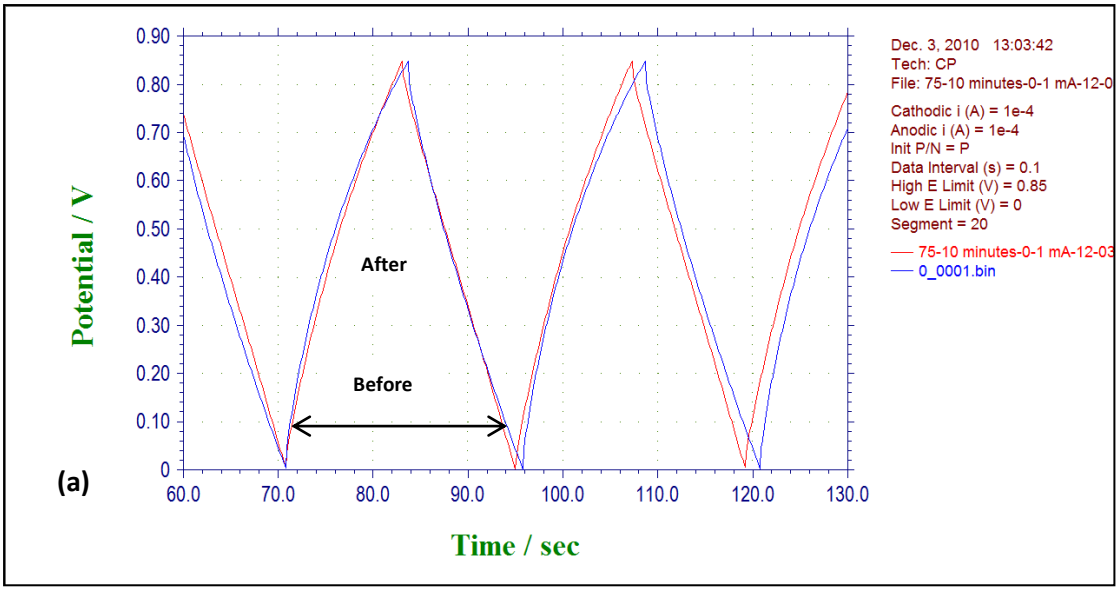

Figure 4.12: Galvanostatic charge/discharge cycles at current density of 100 μA cm^{-2}.

As shown in Figure 4.12, the charging time of the CNTs electrode for before and after treatment remained nearly the same. The calculated capacitance was 2764.70μF. Since plasma treatment would act as an etchant on the CNTs, it is expected that the capacitance of CNTs would increase after hydrogen plasma treatment. However, experimental results in Figure 4.13 illustrated that there is no significant change in capacitance. Therefore, hydrogen plasma treatment is not an effective method to modify the CNTs capacitance.

CHAPTER IV

SUMMARY AND CONCLUSIONS

In this research, vertically aligned multiwalled CNTs have been synthesized by hot filament chemical vapor deposition (HFCVD) method. It was clearly seen that process parameters such as growth time, flow rates, gas combinations affect CNT growth. It is also seen that ammonia controls the alignment and quality of CNTs. The height of the CNTs ranges from 6-50 μm with various growth times such as 2 min, 4 min, 6 min, 8 min, and 10 min were obtained. Moreover, the as grown CNT samples fabricated in higher ammonia concentration environment provided a better electrode capacitance values compared to those fabricated in lower ammonia ambient. Overall, the results illustrated thus far, in the first part of research, show that aligned CNTs can be grown under different parameters and conditions by HFCVD method. Higher density of vertically aligned CNTs gives more effective surface area for supercapacitors applications.

In the second part of the research, the as grown CNTs electrodes were characterized for supercapacitor application. Post synthesis treatment of CNTs including polyvinyl alcohol (PVA) treatment, H_2O_2 (hydrogen peroxide) treatment, H_2 (hydrogen) plasma treatment, were performed and used to improve the CNTs electrodes capacitance. Supercapacitor characteristics such as charging/discharging, and impedance (Z) characteristics were also examined. The encouraging results demonstrated that polyvinyl alcohol (PVA) could be used to functionalize carbon nanotubes and transform the nature hydrophobic nanotube surfaces into desirable

hydrophilic surface to enhance the capacitive performance. In addition, charge/discharge characteristic and impedance measurement supported these desirable results. On the other hand, hydrogen peroxide treatment was found not to be a useful method for modifying the carbon nanotubes for ultracapacitor application. In the final part of the research, hydrogen plasma treatment was used for removal of amorphous carbon and metal nanoparticles from CNTs surface to obtain relatively higher specific surface area. Even though most of the amorphous carbon is removed by hydrogen plasma treatment, there is no visible change in capacitance behavior of CNTs based electrode.

CHAPTER V

RECOMMENDATIONS

The results of CNT synthesis by hot filament chemical vapor deposition (HFCVD) have shown desirable carbon nanotube structure. Furthermore, electrochemical characterization of CNTs based electrode with various chemical treatment such as polyvinyl alcohol, hydrogen peroxide, and hydrogen plasma treatment have also shown different aspect for CNT based supercapacitors. Nevertheless, there is a huge range of improvement in the performance of carbon nanotube based supercapacitors. The future studies will include following:

- Perform transmission electron microscopy (TEM) analysis of the CNTs to investigate the actual tube diameter, metal particles and amorphous carbon.
- Perform Raman spectra and XPS analysis of the as grown and treated CNTs.
- Using different catalyst such as Fe, Ni, Pd, and Mo in the HFCVD of CNTs.
- Investigate the effect of different chemical oxidative treatments such as sulfuric acid, nitric acid, permanganate, nitric acid-sulfuric acid mixture.
- Investigate the effect of using different conducting polymers treatment such as polyvinyl, polyacetylene, polypyrrole, and polyaniline.
- Determine the different electrolyte impression for capacitance behavior.

REFERENCES

[1] http://en.wikipedia.org/wiki/Carbon_nanotube

[2] M. Meyyappan, Carbon Nanotubes Science and Applications, CRC Press, 2-21

[3] M. Dresselhaus, G. Dresselhaus, and P. Eklund, Science of Fullerenes and Carbon Nanotubes, Academic Press, San Diego (1996)

[4] Caterina Leone, "High Performance Synthesis and Purification of Carbon Nanotubes", Department of Chemical and Food Engineering of the University of Salerno

[5] Nikkon Ghosh, "CNT Field Emission Cell with Built-in Electron Beam Source for Electron Stimulated Amplified Field Emission", Electrical Engineering & Computer Science of Vanderbilt University, August 2008

[6] M. Dresselhaus, G. Dresselhaus, and Phaedon Avouris, Carbon Nanotubes Synthesis, Structure, Properties, and Applications, Springer, 1-20

[7] Hari Singh Nalwa, George A. Olah, Handbook of Nanostructured Materials and Nanotechnology, Organics, Polymers, and Biological Materials (5), Academic Press, 375-403

[8] J.H. Chen, W.Z. Li, D.Z. Wang, S.X. Yang, J.G Wen, Z.F. Ren, Carbon 40 (2002) 1193-1197

[9] Che G, Lakshmi BB, Martin CR, Fisher ER. Langmuir

[10] Kong J, Franklin NR, Zhou C, Chapline MG, Peng S, Cho K et al. Science 2000;287:622.

[11] Dillon AC, Jones KM, Bekkedahl TA, Kiang CH, Bethune DS, Heben MJ. Nature 1997;386:377.

[12] Wildoer J, Venema L, Rinzler A, Smalley R, Dekker C Nature 1998;391:59

[13] W.B. Choi, D.S. Chung, J.H. Kang, H.Y. Kim, Y.W. Jin, I.T. Han, Y.H. Lee, J.E. Jung, N.S. Lee, G.S. Park, J.M. Kim, Appl. Phys. Lett. 75 (1999) 3129

[14] J. Robertson, W.I. Milne, K.B.K. Teo, M. Chhowalla, "Field emission application of carbon nanotubes", XVI International Winterschool on Electronic Properties of Novel Materials, Kirchberg, Austria, 2002 (2–9 March), pp. 537–542

[15] Y.M. Wong, W.P. Kang, J.L. Davidson, A. Wisitsora-at, K.L. Soh, Sens. Actuators, B 93 (2003) 326–331

[16] J. Hafner, C. Cheung, C. Lieber, Nature 398 (1999) 761

[17] S.J. Tans, M.H. Devoret, H. Dai, A. Thess, R.E. Smalley, L.J. Geerlings, C. Dekker, Nature 386 (1997) 474

[18] C. Lui, Y.Y. Fan, M. Lui, H.T. Cong, M.S. Dresselhaus, "Hydrogen storage in single walled carbon nanotubes at room temperature", Science 286 (1127) (1999)

[19] R. Rosen, W. Simendinger, C. Debbault, H. Shimoda, L. Fleming, B. Stoner, and O. Zhuo, Appl. Phys. Lett. 76 (2000) 1668-1670

[20] C. Nui, E. K. Sichel, R. Hoch, D. Moy, and H Tennent, Appl. Phys. Lett. 70 (1997) 1480

[21] T. Rueckes, K. Kim, E. joselevich, G. Y. Tseng, C. L. Cheung, and C. M. Lieber, Science 289 (2000) 94-97

[22] P. Kim and C. M. Lieber, Science 286 (1999) 2148-2150

[23] S.J. Wind, J. Appenzeller, R. Martel, and P. Avouris, "Vertical scaling of carbon nanotube field effect transistors using top gate electrodes", Appl. Phys . Lett. 80 (2002) 3817

[24] F. Javier del Campo, J Garcia – Cespedes, F. Xavier Munoz, E. Bertran, Electrochemistry Communications 10 (2008) 1242- 1245

[25] Chongfu Zhou, "Carbon Nanotube Based Electrochemical Supercapacitors", School of Polymer, Textile and Fiber Engineering, Georgia Institute of Technology, December, 2006

[26] Chunsheng Du and Ning Pan, Nanotechnology Law & Business, March 2007

[27] http://nuin.co.kr/

[28] http://e-articles.info/e/a/title/Advantages-and-Disadvantages-of-Supercapacitor/

[29] A. Rudge, I. Raistrick, S. Gottesfeld, J. P. Ferraris. Electrochim. Acta 1994, 39, 273.

[30] E. Frackowiak, K. Jurewicz, S. Delpeux, F. Beguin. J. Power Sources 2001, 97-98, 822.

[31] D. Belanger, X. Ren, J. Davey, F. Uribe, S. Gottesfeld. J. Electrochem. Soc 2001, 147, 2923

[32] J. M Boyea, R.E. Camacho, S.P. Turano, and W.J. Ready, Nanotechnology Law & Business, March 2007

[33] E. Frackowiak, F. Beguin. Carbon 2001, 39 (6), 937.

[34] J. Y. Lee, K. H. An, J. K. Heo, Y. H. Lee. J. Phys. Chem. B 2003, 107, 8812.

[35] B.-J. Yoon, S.-H. Jeong, K.-H. Lee, H.-S. Kim, C. G. Park, J. H. Han. Chem. Phys. Lett**.** 2004, 388, 170-174.

[36] Fa-Kuei Tung, Masamichi Yoshimura, Kazuyuki Ueda, Yutaka Ohira, Takayoshi Tanji, Applied Surface Science 254 (2008) 7750-7754

[37] Amjad H. El-Sheikh, *Jordan Journal of Chemistry* Vol.3 No.3, 2008, pp. 293-304

[38] http://www.grc.nasa.gov/WWW/RT/2006/RX/RX24P-lebron.html

[39] Hong-Zhang Geng, Ki Kang Kim, Kang Pyo So, Young Sil Lee, Youngkyu Chang, and Young Hee Lee, *J.Am Chem. Soc.*, Vol. 129, No. 25, 2007, 7759

[40] Patrice Simon, Andrew Burke, Nanostructured carbons: Double Layer Capacitance and More, The Electrochemical Society Interface, Spring 2008, 38-45

[41] V. Shanov, Yeo-Heung Yun, M. J. Schulz, *Journal of the University of Chemical Technology and Metallurgy*, 41, 4, 2006, 377-390

[42] http://en.wikipedia.org/wiki/Carbon_nanotube

[43] Richard C. Jaeger, Introduction to Microelectronic Fabrication, Second Edition, Volume 5, 10-100

[44] http://en.wikipedia.org/wiki/Ammonium_fluoride

[45] Cynthia G. Zoski, Handbook of Electrochemistry, New Mexico State University Department of Chemistry and Biochemistry, 2007 Elsevier

[46] http://en.wikipedia.org/wiki/Cyclic_voltammetry

[47] Supil Raina, W. P. Kang, J. L Davidson, Diamond & Related Materials 17 (2008) 896 – 899

[48] S. Wei, W. P. Kang, J. L Davidson, J.H. Huang, Diamond & Related Materials 17 (2008) 906-911

[49] Chijuan Hu, "Fluid Coke Derived Activated Carbon as Electrode Material for Electrochemical Double Layer Capacitor", Graduate Department of Chemical Engineering and Applied Chemistry, University of Toronto, 2008

[50] Yun Peng and Hewen Liu, Ind. Eng. Chem. Res. 2006, 45, 6483-6488

[51] Harindra Vedala, Jun Huang, Xiang Yang Zhou, Gene Kim, Somenath Roy, Won Bong Choi, Applied Surface Science 252 (2006) 7987-7992

[52] V.Datsyuk, M. Kalyva, K. Papagelis, J. Parthenios, D. Tasis, A. Siokou, I. Kallitsis, C. Galiotis, Carbon 46 (2008) 833-840

[53] M. Vesali Naseh, A. A. Khodadadi, Y. Mortazavi, O. Alizadeh Sahraei, F. Pourfayaz, and S. Mosadegh Sedghi, World Academy of Science, enginnering and Technology 49 2009

[54] Yasumitsu Miyata, Yutaka Maniwa, and Hiromichi Kataura, "Selective Oxidation of Semiconducting Single- Wall Carbon Nanotubes by Hydrogen peroxide", the Journal of Physical Chemistry B Letters, 2006, 110, 25-29

[55] S. R. C. Vivekchand, A. Govindaraj, Md. Motin Seikh, and C. N. R. Rao, *J. Phys. Chem. B* 2004, 108, 6935-6937

[56] Leimei Sheng, Lei Shi, Kang An, Liming Yu, Yoshinori Ando, Xinluo Zhao, Chemical Physics Letters 502 (2011) 101-106

[57] H. Z. Wang, Z. P. Huang, Q. J. Cai, K. Kulkarni, C.-L Chen, D Carnahan, Z. F. Ren, Carbon 48 (2010) 868-875

[58] S. R. S. Prabaharan, R. Vimala, Zulkarnian Zainal, " Nanostructured Mesoporous Carbon as Electrode for Supercapacitors",School of Electrical and Electronics Engineering, The university of Nottingham Malaysia Campus, 27-28 March 2006,

[59] C. Portet, P. L. Taberna, P. Simon, E. Flahaut, C. Laberty-Robert, Electrochimica Acta 50 (2005) 4174-4181